

DIS97

Chicago, Illinois, USA

April 14-18, 1997

H1 Results in Deep Inelastic Scattering

Gregorio Bernardi

LPNHE-Paris,
CNRS-IN2P3

On behalf of the

H1 Collaboration



~

Outlay

- H1 and HERA

- Diffraction

$F_2^{D(3)}$ and QCD

Vector Mesons

- Hadronic Final State

α_S as determined by event shapes in DIS

Hadronic final state at low x

- Structure Functions

F_2 at low Q^2

QCD interpretations

- High Q^2 physics

Differential cross-sections in CC and NC

Did you say LeptoQuarks?

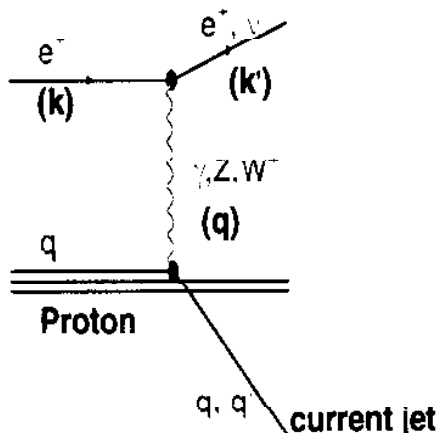
- Summary

Points Treated Only in Parallel Sessions:

- Diffractive processes with leading neutrons :
D. Jansen / WG2
- Energy Flow, Thrust, Charm in DIS :
C Cormack / WG2
- Diffractive Jet Production :
P. Marage / WG2
- Diffractive Photoproduction in H1 :
P. Newman / WG2
- Photoproduction jet results + Virtual photon structure:
T. Ebert / WG3
- Multiplicities / Bose Einstein Correlations :
P. Van Mechelen / WG2
- Bose-Einstein Correlations in DIS :
M. Charlet / WG3
- Review of instanton searches at HERA :
T. Carli / WG3
- Search for Odderons :
S. Tapprogge / WG2
- Breit-frame studies: fragm. and scaling violations :
A. De Roeck / WG3
- On the α_S measurement :
M. Weber / WG1+WG3
- Inelastic J/Psi prod. and determ. of gluon density :
A. Wegner / WG3
- QCD fits, $F_2^{c\bar{c}}$ and F_L + Jet rates and the Gluon density :
F. Zomer / WG3

Introduction

At HERA, the proton can be probed at very small distances
 $(\simeq 10^{-16}\text{cm})$, e.g. t -channel exchange of virtual gauge bosons



$$Q^2 = -q^2$$

$$x = Q^2/(P \cdot q)$$

$$y = (P \cdot q)/(P \cdot k)$$

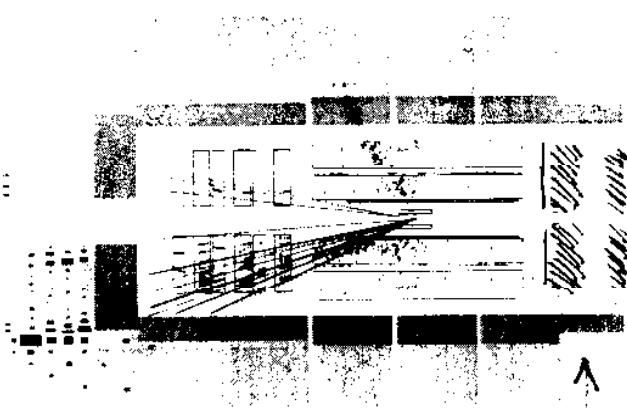
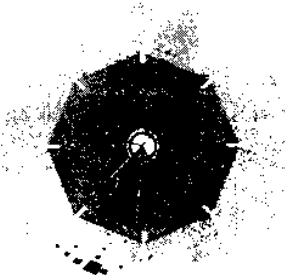
$$W = \sqrt{Q^2(1-x)/x} \simeq ys$$

$$M = \sqrt{sx} = \sqrt{Q^2/y}$$

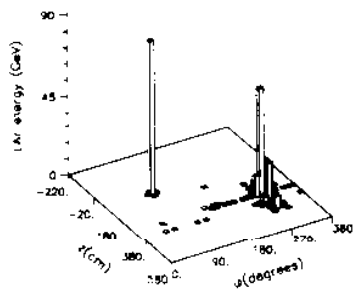
Run 181127 Event 2488 Class: 2 8 9 18 20 22 26 Date: 3/04/1997

1997!
event

$M \simeq 200\text{ GeV}$

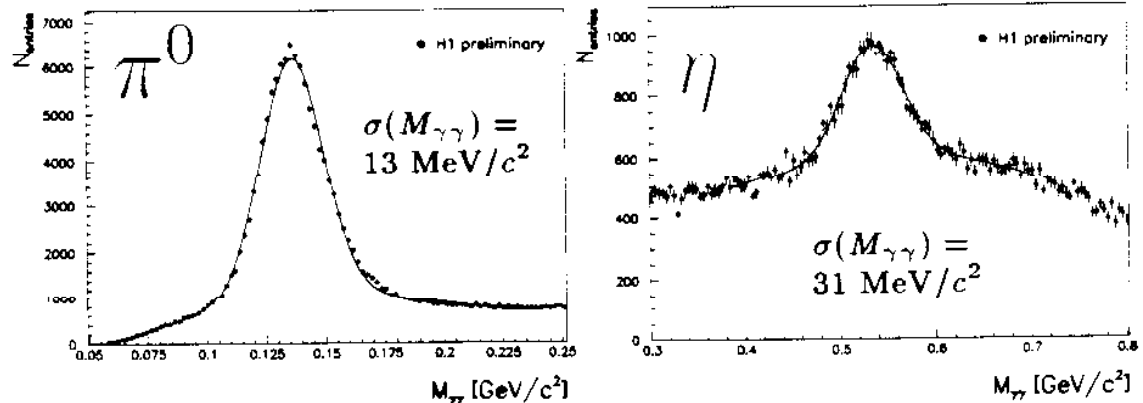


Upgraded
in '95



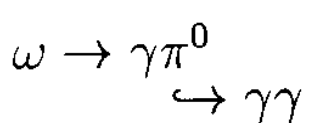
The SPACAL Performance

Tagged photoproduction ($0.3 < y < 0.7, Q^2 < 0.01 \text{ GeV}^2/c^2$)

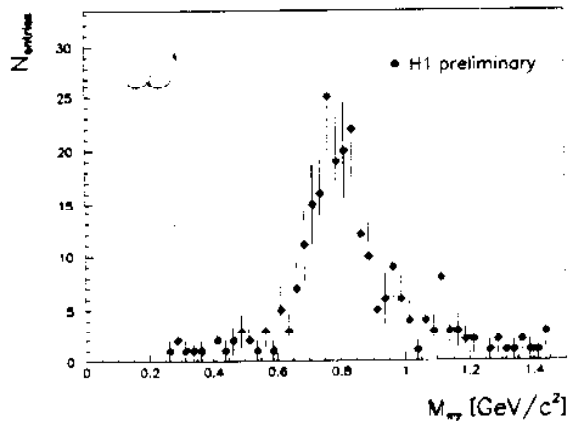


New detector: SPACAL (SPAGhetti CALorimeter)

- lead/scintillating-fibre matrix (photomultiplier readout)
- wider angular acceptance: $153^\circ < \vartheta < 177.5^\circ$
- lower energy threshold ($\approx 100 \text{ MeV}$), timing capabilities
- fine granularity: cell size $4 \times 4 \text{ cm}^2$
- very good energy resolution: $\sigma/E = 7\%/\sqrt{E/\text{GeV}} \oplus 1\%$

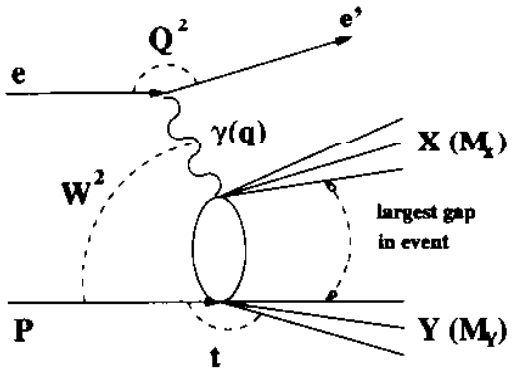


B.R. = 8.5 %



Diffraction at HERA

DIS Events characterized by the exchange of a colourless particle
⇒ large rapidity gap in the hadronic final state



Additional variables in terms of systems X and Y:

$$\begin{aligned}\beta &= \frac{Q^2}{2q \cdot (P - Y)} \approx \frac{Q^2}{Q^2 + M_X^2} \\ &\Rightarrow x_{Bj} = \beta \cdot x_P \\ x_P &= \frac{q \cdot (P - Y)}{q \cdot P} \approx \frac{Q^2 + M_X^2}{Q^2 + W^2}\end{aligned}$$

Interpretation in terms of exchange:

- | | |
|---------|--|
| x_P | momentum fraction of exchange particle |
| β | momentum fraction of parton |

Kinematic Range:

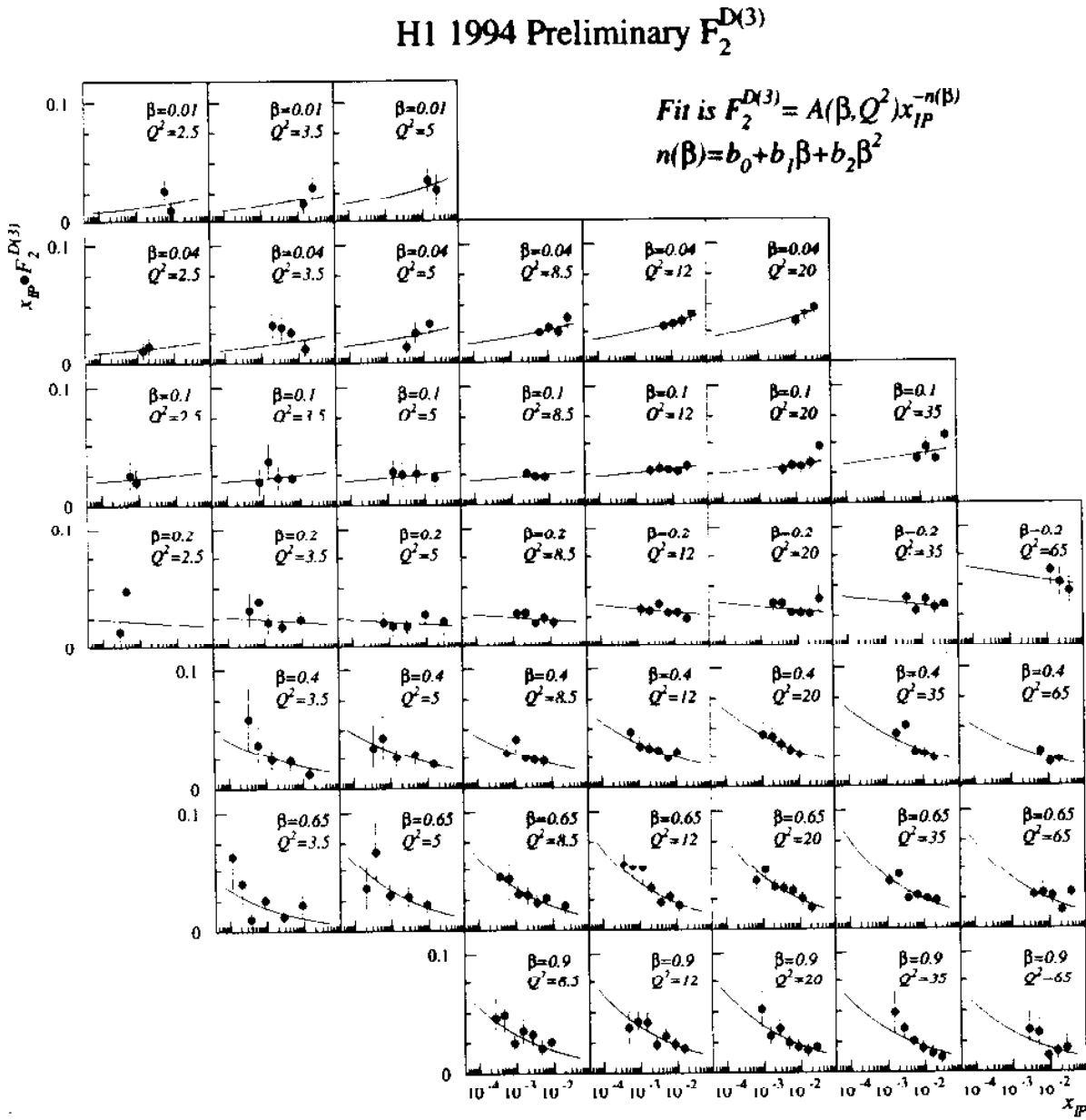
$$\begin{aligned}2.5 < Q^2 &< 65 \text{ GeV}^2 \\ 0.01 < \beta &< 0.9 \\ 0.0001 < x_P &< 0.05\end{aligned}$$

$$\begin{aligned}t &\lesssim -1 \text{ GeV}^2 \\ M_Y &\lesssim 1.6 \text{ GeV}\end{aligned}$$

Measured differential cross-section ⇒ $F_2^{D(3)}(Q^2, \beta, x_P)$

$$\frac{d^3\sigma_{ep \rightarrow e\ell XY}^D}{d\beta dQ^2 dx_P} = \frac{4\pi\alpha^2}{\beta Q^4} \left(1 - y + \frac{y^2}{2}\right) \cdot F_2^{D(3)}(Q^2, \beta, x_P)$$

H1 1994 Observation of Factorisation Breaking



Breaking of experimental factorisation !

$$F_2^{D(3)} = A(\beta, Q^2) \cdot x_{IP}^{-n(\beta)}$$

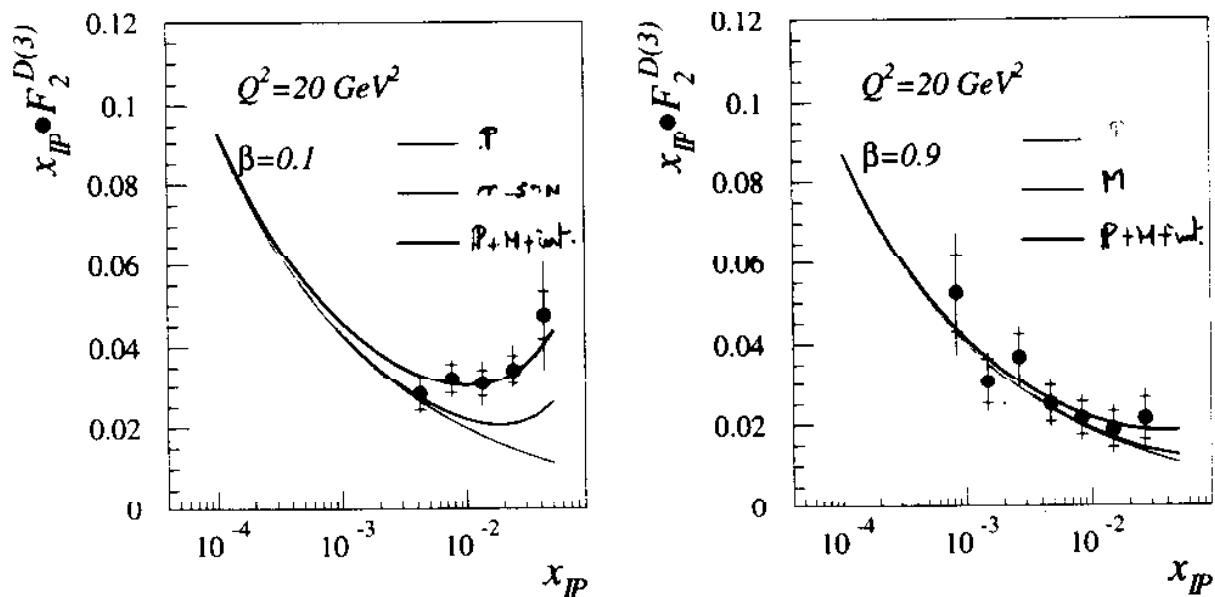
High β - $n \sim 1.25$

Low β - $n \sim 1$ or less

lit F_2^P

Pomeron + Meson

H1 Preliminary 1994



fit of $F_2^P(\beta, Q^2)$, n_1 , C_M , n_2 :
 $n_1 = 1.29 \pm .03$ $n_2 = 0.3 \pm .3$

$$F_2^P(x_P, \beta, Q^2) = \frac{r_P}{x_P^n} (\beta, Q^2) x_P^{-n_1} + C_M F_2^M x_P^{-n_2} + \text{fut}$$

$$\chi^2/ndf = 170/156$$

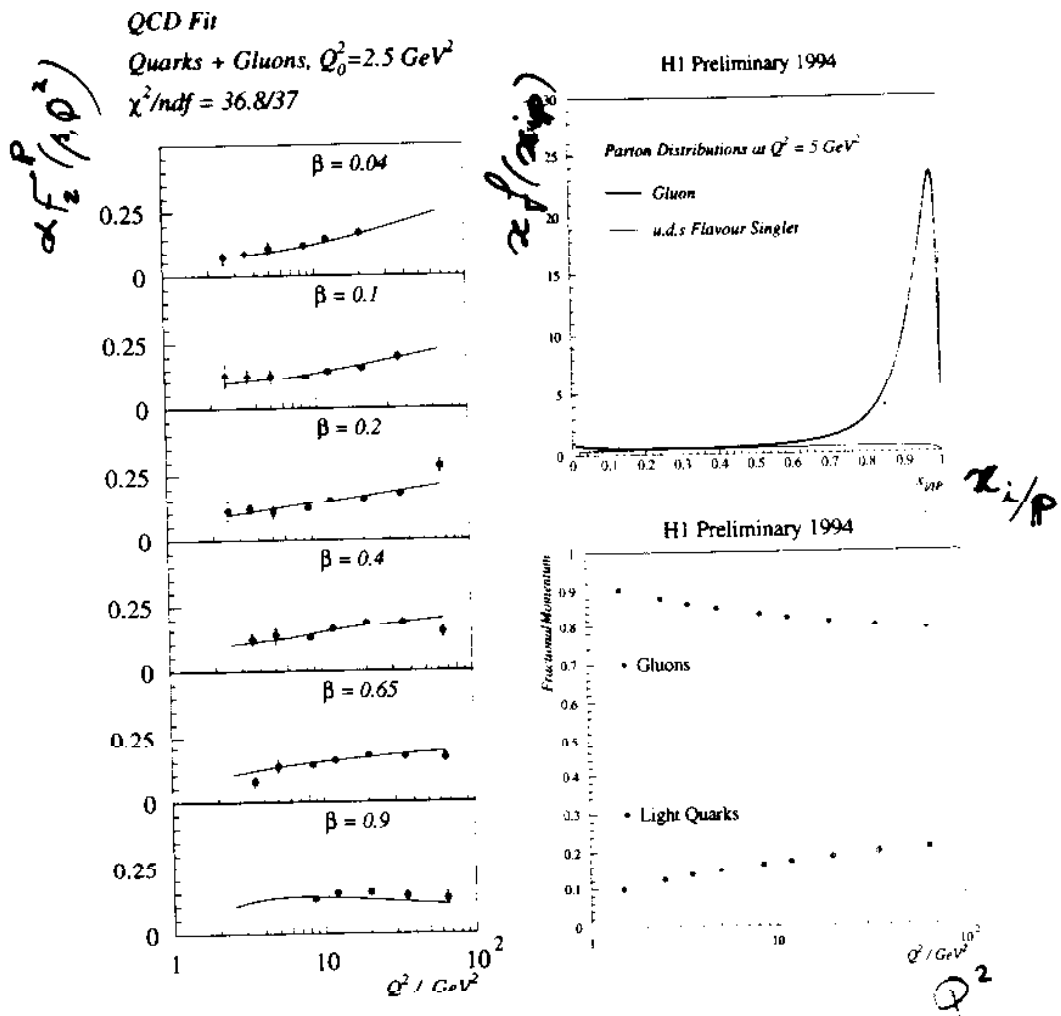
assuming peripheral t -dependence ($\propto e^{bt}$)
 and linear trajectories $\alpha(t) = \alpha(0) + \alpha' \cdot t$

$$\begin{array}{ll} b_M = 5, \alpha'_M = 1 & \alpha_M(0) = 0.6 \pm 0.1 \pm 0.3 \\ \alpha'_P = 0 & \alpha_P(0) = 1.15 \pm 0.02 \pm 0.04 \\ \alpha'_P = 0.3, b_P = 6 & \alpha_P(0) = 1.18 \pm 0.02 \pm 0.04 \end{array}$$

- large meson contribution at small β and high x_P
- few % meson intensity for $x_P < 0.01$
- large contribution of interference

Partonic Structure of Diffractive Exchange

$$F_2^{D(3)}(\beta, Q^2, x_{IP}) = f_{IP/p}(x_{IP}, t) \cdot \tilde{F}_2^P(\beta, Q^2)$$

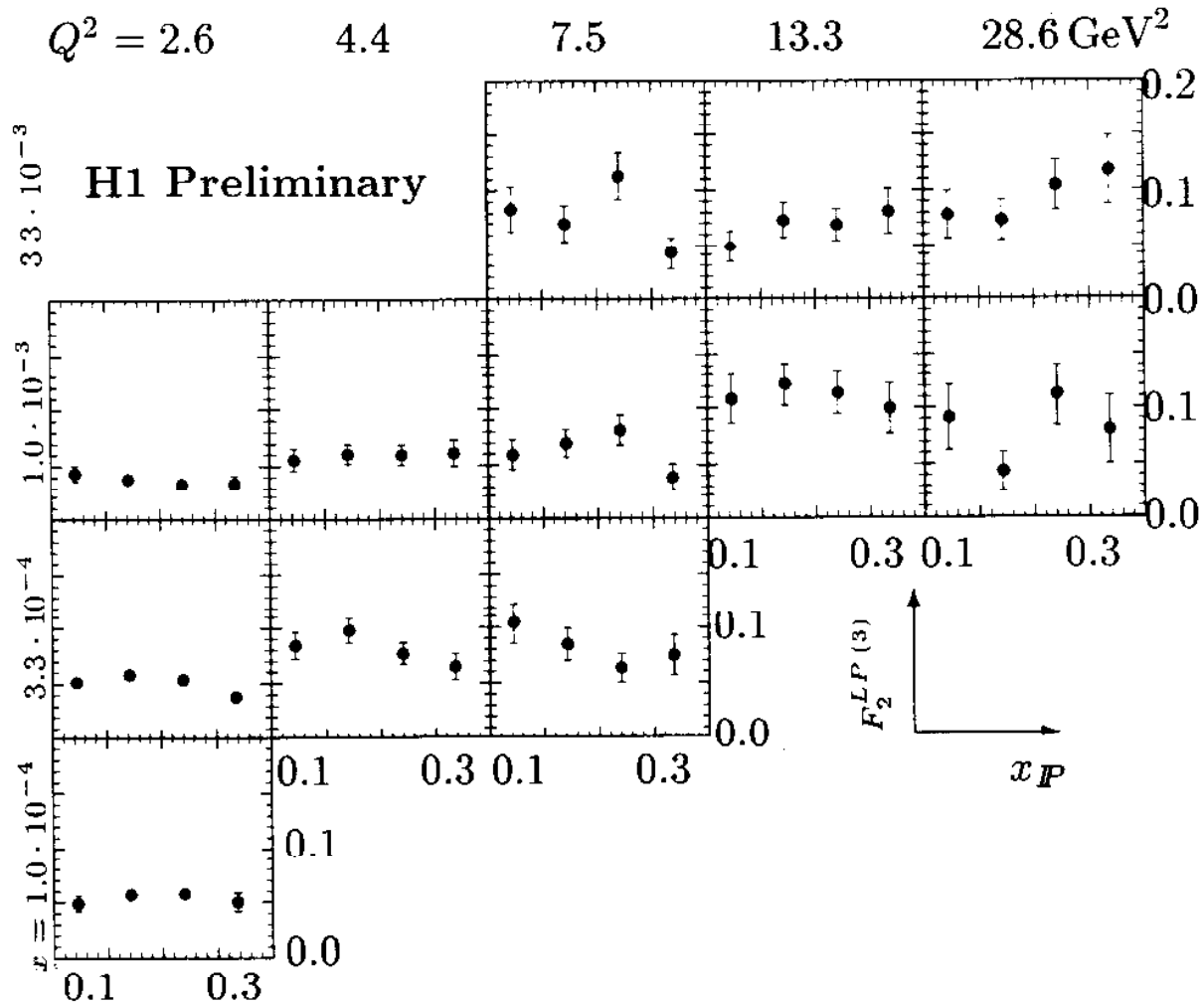


- \tilde{F}_2^D Shows no evidence of a fall in Q^2 with increasing β
- Strong Q^2 scaling violations \rightarrow very hard gluon density?
- DGLAP QCD fit including Quarks and Gluons at the starting scale gives best fit, Quark only gives a poor fit
- “Leading Gluon” gluon behaviour seen $x_g/IP \rightarrow 1$ as $Q^2 \sim Q_0^2$
- Significant fraction of the Pomeron’s momentum is carried by gluons

DIS with Leading Protons in the Forward Proton Spectrometer

- Selection: DIS events with protons of $p_T < 200$ MeV measured with the Forward Proton Spectrometer.
- Energy range $E'_p = 580 - 740$ GeV
 \Rightarrow new kinematic domain $x_F = 1 - E'_p/E_p = 0.1 - 0.3$.
- Parametrized by semi-inclusive structure function $F_2^{LP(3)}$:

$$\frac{d^3\sigma(ep \rightarrow e'p'X)}{dx_F dQ^2 dx_F} = \frac{4\pi\alpha^2}{x Q^4} \left(1 - y + \frac{y^2}{2}\right) F_2^{LP(3)}(x, Q^2, x_F)$$



B. List W6²

Vector Mesons

- Different theoretical predictions for the dependence on kinematic variables of the differential cross sections
 - Regge phenomenology – pomeron exchange
 - perturbative QCD calculations
- Analysed decay modes

$$\begin{aligned}\rho^0 &\rightarrow \pi^+ \pi^- \\ \phi &\rightarrow K^+ K^- \\ J/\Psi &\rightarrow l^+ l^- (l = e, \mu)\end{aligned}$$

- Study transition region from soft to hard physics on 2 scales:
mass of the vector meson and virtuality of the photon Q^2
- Dependence on kinematic variables:
 - $W_{\gamma p}$

$$\frac{d\sigma}{dt} \Big|_{t=0} \propto W_{\gamma p}^{4*0.0808} \quad \text{REGGE}$$

$$\frac{d\sigma}{dt} \Big|_{t=0} \propto \frac{[x G(x, Q)]^2}{Q^6} \quad \text{pQCD}$$

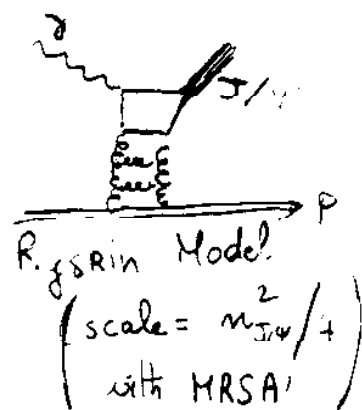
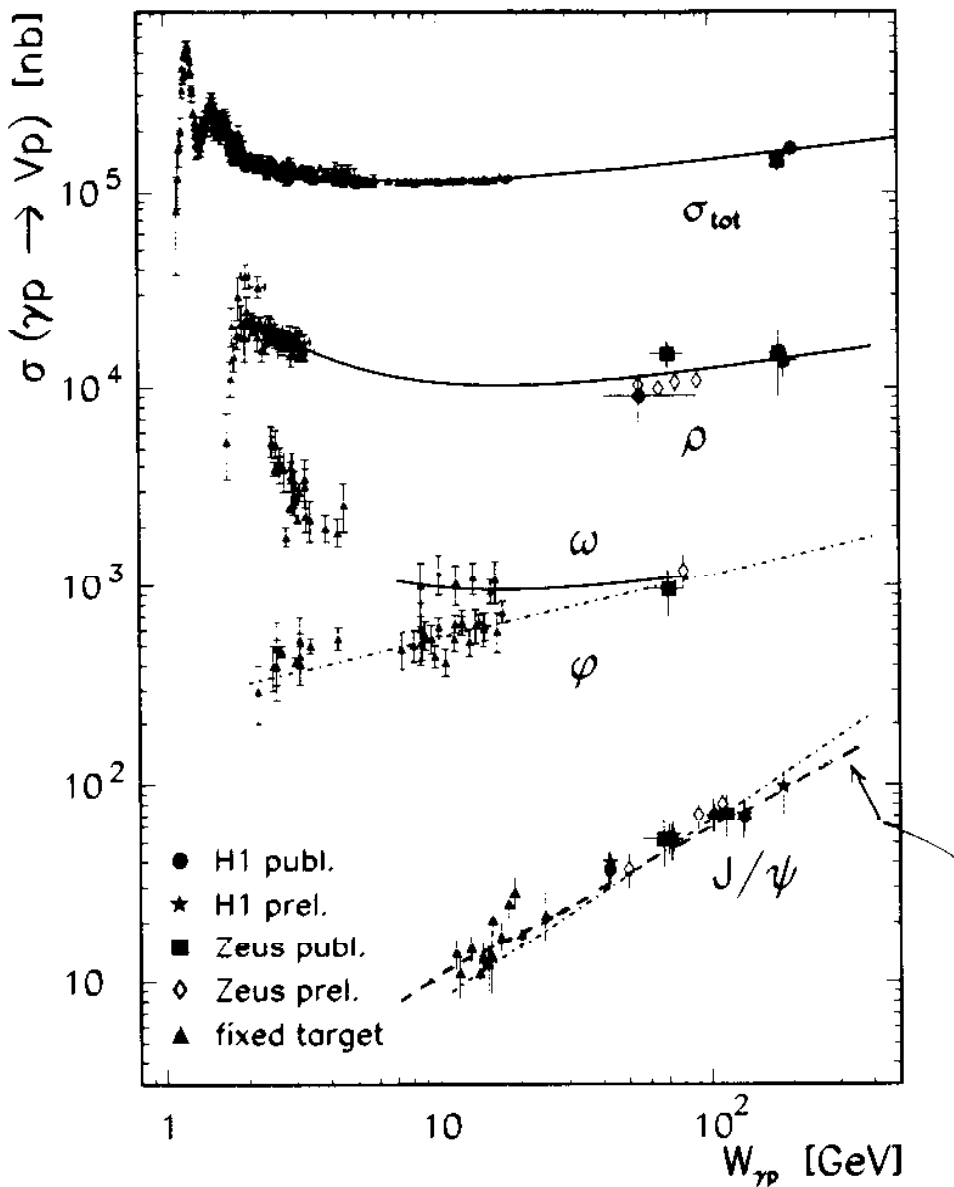
$$W_{\gamma p}^2 - \frac{1-x}{x} Q^2 \rightarrow \text{steep rise with } W$$

$$- Q^2$$

$$\frac{d\sigma}{dQ^2} \propto (m_{VM}^2 + Q^2)^{-n} \quad \text{REGGE VDM}$$

F. Gaede, W

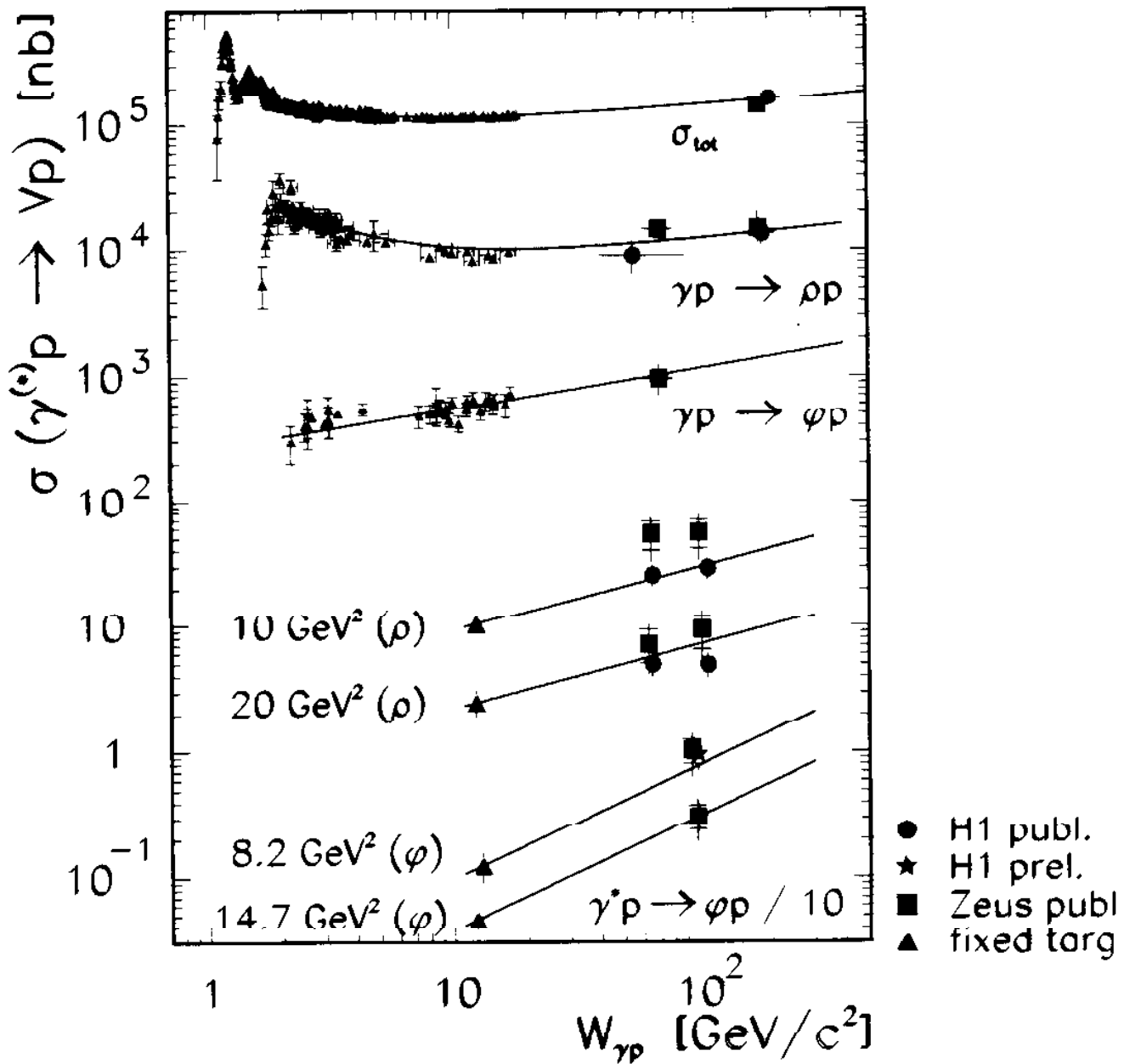
photoproduction elastic cross sections



- light vector mesons described by soft pomeron
- J/Ψ steeper rise \rightarrow 'hard' pomeron

Ryskin

$W_{\gamma p}$ dependence: ρ^0 vs Φ



- Φ : steeper rise with $W_{\gamma p}$ than in photoproduction
- increase larger for Φ than for ρ^0
harder scale due to larger mass

Summary on Diffraction

- 1

- $F_2^{D(3)}$ has been measured and QCD analyzed at low Q^2
 - Evidence for factorisation breaking in β which may be interpreted as due to presence of meson exchange at high x_{IP} and small β .
 - QCD analysis indicates a strong content of gluons in the IP with a density peaking at high $x_{i/PI}$
 - Energy Flow and open Charm have been measured in deep-inelastic diffraction and support the gluon dominated interpretation of the IP (not shown)
 - Leading Proton $F_2^{LP(3)}$ has been measured in a new kinematic domain
 $\Rightarrow 0.1 < x_{IP} < 0.3$
- Vector Mesons
 - photoproduction
 - * slow rise of $\sigma_{\gamma p}$ with $W_{\gamma p}$ for the ρ^0 well described by soft pomeron
 - * steeper rise for the J/Ψ , now seen from HERA data alone
 \rightarrow best evidence yet for 'hard' pomeron
 - high Q^2
 - * Φ and J/Ψ show steeper rise with $W_{\gamma p}$ at high Q^2 but still depending on low energy data
 \rightarrow need $W_{\gamma p}$ dependence from HERA data alone

Model in which Pomeron's momentum is carried largely by gluons reproduces all aspects of Diffractive Scattering

- Phase Space in the Current Hemisphere of the Breit Frame for $e p \rightarrow e X$ Events:

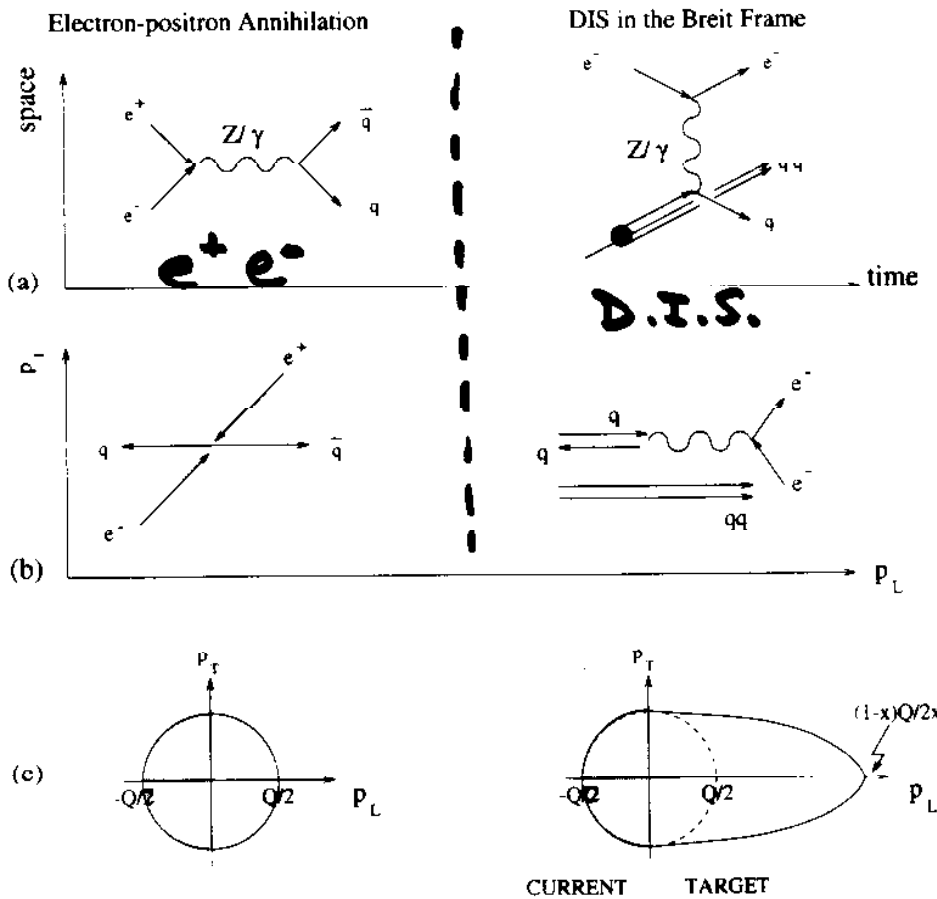
$$Q/2$$

- Phase Space in one Hemisphere of $e^+ e^- \rightarrow q \bar{q}$ Events:

$$\sqrt{s}/2$$

\Rightarrow Is there a relation between $e p$ Scattering and $e^+ e^-$ Annihilation concerning Event Shapes at a Scale:

$$Q_{DIS} = \sqrt{s_{ee}} ?$$



Power Corrections and $\alpha_s(M_Z)$

- **Q or energy dependence of event shape variables**

- (i) change of strong coupling constant $\alpha_s(Q) \propto 1/\ln(Q/\Lambda)$
- (ii) power or so-called 'hadronisation' corrections $\propto 1/Q$

- **Mean value of any infrared safe event shape variable $\langle F \rangle$**

(e.g. $F = 1 - T_c, (1 - T_z)/2, B_c, \rho_c$)

can be written in DIS $e p$ and in $c^+ c^-$ annihilation as:

$$\langle F \rangle = \langle F \rangle^{\text{pert}} + \langle F \rangle^{\text{pow}}$$

- Perturbative part:

$$\langle F \rangle^{\text{pert}} = c_1 \alpha_s(Q) + c_2 \alpha_s^2(\mu_R)$$

→ coefficients c_1, c_2 from $\mathcal{O}(\alpha_s^2)$ DISENT calculations

- Power corrections:

$$\begin{aligned} \langle F \rangle^{\text{pow}} = a_F \frac{16}{3\pi} \frac{\mu_I}{Q} \ln^p \frac{Q}{\mu_I} & \left[\bar{\alpha}_0(\mu_I) \right. \\ & - \left. \alpha_s(Q) - \frac{\beta_0}{2\pi} \left(\ln \frac{Q}{\mu_I} + \frac{K}{\beta_0} + 1 \right) \alpha_s^2(Q) \right] \end{aligned}$$

[$\bar{\alpha}_0(\mu_I)$ defined at $M_Z^2 \approx W^2$]

→ $\bar{\alpha}_0(\mu_I)$ depends on μ_I (non-perturbative)

$\bar{\alpha}_0(\mu_I) = \bar{\alpha}_0^{\text{pert}} + \delta \bar{\alpha}_0(\mu_I)$

$\bar{\alpha}_0^{\text{pert}} = \text{constant}$ (from DIS)

$\delta \bar{\alpha}_0(\mu_I) = \text{non-perturbative}$ (from $c^+ c^-$ annih.)

→ $\bar{\alpha}_0(\mu_I)$ depends on μ_I (non-perturbative)

→ contain a non-perturbative parameter $\bar{\alpha}_0(\mu_I)$

to be evaluated at some 'infrared matching' scale $\sim \sqrt{\mu_I \alpha_s(Q^2/M_Z^2)}$

- **QCD Analysis of $\langle F \rangle \rightarrow \bar{\alpha}_0$ and $\alpha_s(M_Z)$**

– Power corrections $\propto 1/Q$ for all $\langle F \rangle$

– Universal power correction parameters $\bar{\alpha}_0$ for all $\langle F \rangle$

Event Shape Variables in the Breit Current Hemisphere

- Thrust T_c

$$T_c = \max \frac{\sum_h |\mathbf{p}_h \cdot \mathbf{n}_T|}{\sum_h |\mathbf{p}_h|} \quad \mathbf{n}_T \equiv \text{thrust axis}$$

- Thrust T_z closer to $e^+ e^-$ annihilation

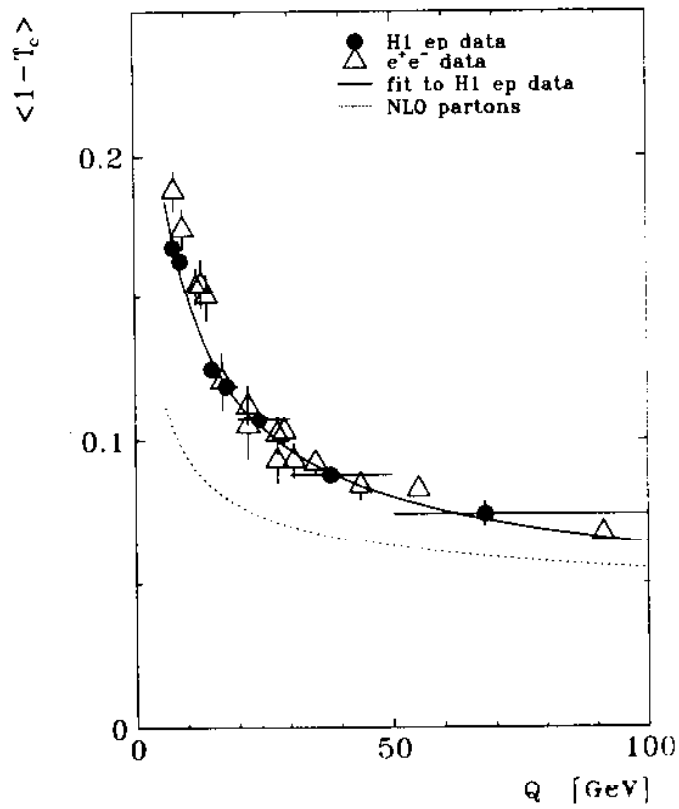
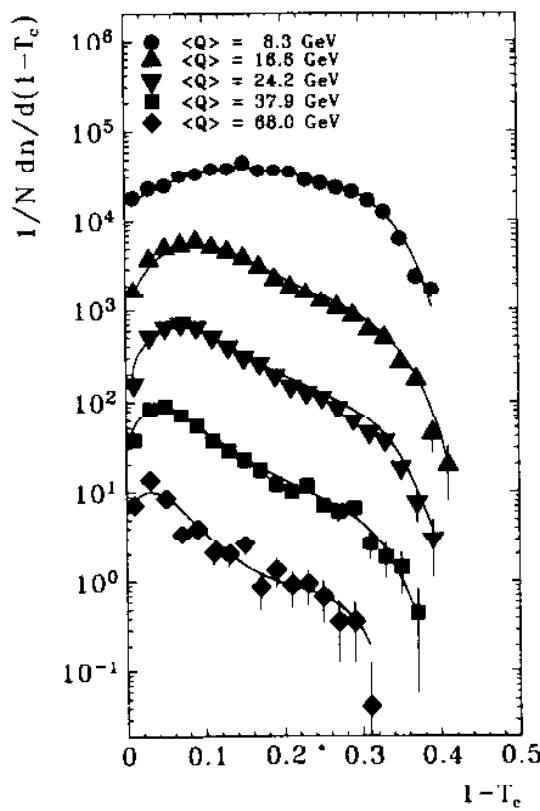
$$T_z = \frac{\sum_h |\mathbf{p}_h \cdot \mathbf{n}|}{\sum_h |\mathbf{p}_h|} = \frac{\sum_h |\mathbf{p}_{zh}|}{\sum_h |\mathbf{p}_h|} \quad \mathbf{n} \equiv \text{hemisphere axis}$$

- Jet Broadening B_c

$$B_c = \frac{\sum_h |\mathbf{p}_h \times \mathbf{n}|}{2 \sum_h |\mathbf{p}_h|} = \frac{\sum_h |\mathbf{p}_{\perp h}|}{2 \sum_h |\mathbf{p}_h|} \quad \mathbf{n} \equiv \text{hemisphere axis}$$

- Jet Mass ρ_c

$$\rho_c = \frac{M^2}{Q^2} = \frac{(\sum_h p_h)^2}{Q^2}$$



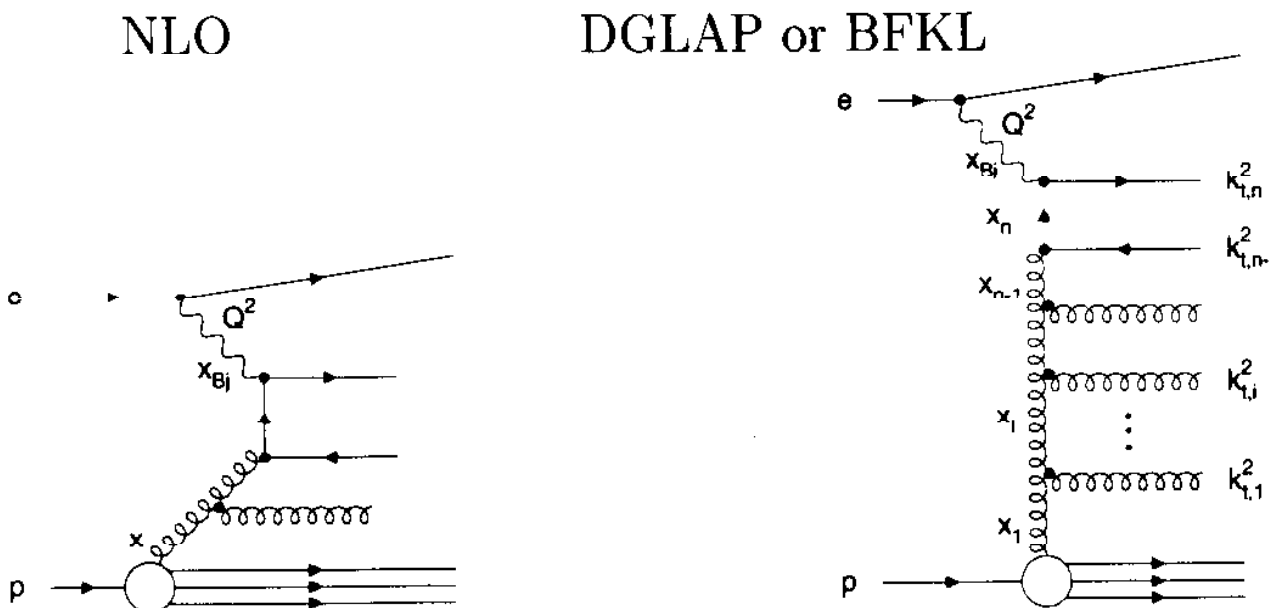
Results of QCD fits and Conclusions

Observable	$\bar{\alpha}_0(\mu_I = 2 \text{ GeV})$	$\alpha_s(M_Z)$	χ^2/ndf
<hr/>			
H1 $e p$ data			
$\langle 1 - T_c \rangle$	$0.497 \pm 0.005 \stackrel{+0.070}{-0.036}$	$0.123 \pm 0.002 \stackrel{+0.007}{-0.005}$	$5.0/5$
$\langle 1 - T_z \rangle / 2$	$0.507 \pm 0.008 \stackrel{+0.109}{-0.051}$	$0.115 \pm 0.002 \stackrel{+0.007}{-0.005}$	$8.5/5$
$\langle B_c \rangle$	$0.408 \pm 0.006 \stackrel{+0.036}{-0.022}$	$0.119 \pm 0.003 \stackrel{+0.007}{-0.004}$	$5.3/5$
$\langle \rho_c \rangle$	$0.519 \pm 0.009 \stackrel{+0.025}{-0.020}$	$0.130 \pm 0.003 \stackrel{+0.007}{-0.005}$	$3.1/5$
<hr/>			
common fit			
$T_c + T_z + \rho_c$	$0.491 \pm 0.003 \stackrel{+0.079}{-0.042}$	$0.118 \pm 0.001 \stackrel{+0.007}{-0.006}$	$39/11$
<hr/>			
e^+e^- data			
$\langle 1 - T_{ee} \rangle$	$0.519 \pm 0.009 \stackrel{+0.093}{-0.039}$	$0.123 \pm 0.001 \stackrel{+0.007}{-0.004}$	$10.9/5$
$\langle M_H^2/s \rangle$	$0.580 \pm 0.015 \stackrel{+0.130}{-0.053}$	$0.119 \pm 0.001 \stackrel{+0.004}{-0.003}$	$10.9/5$
<hr/>			

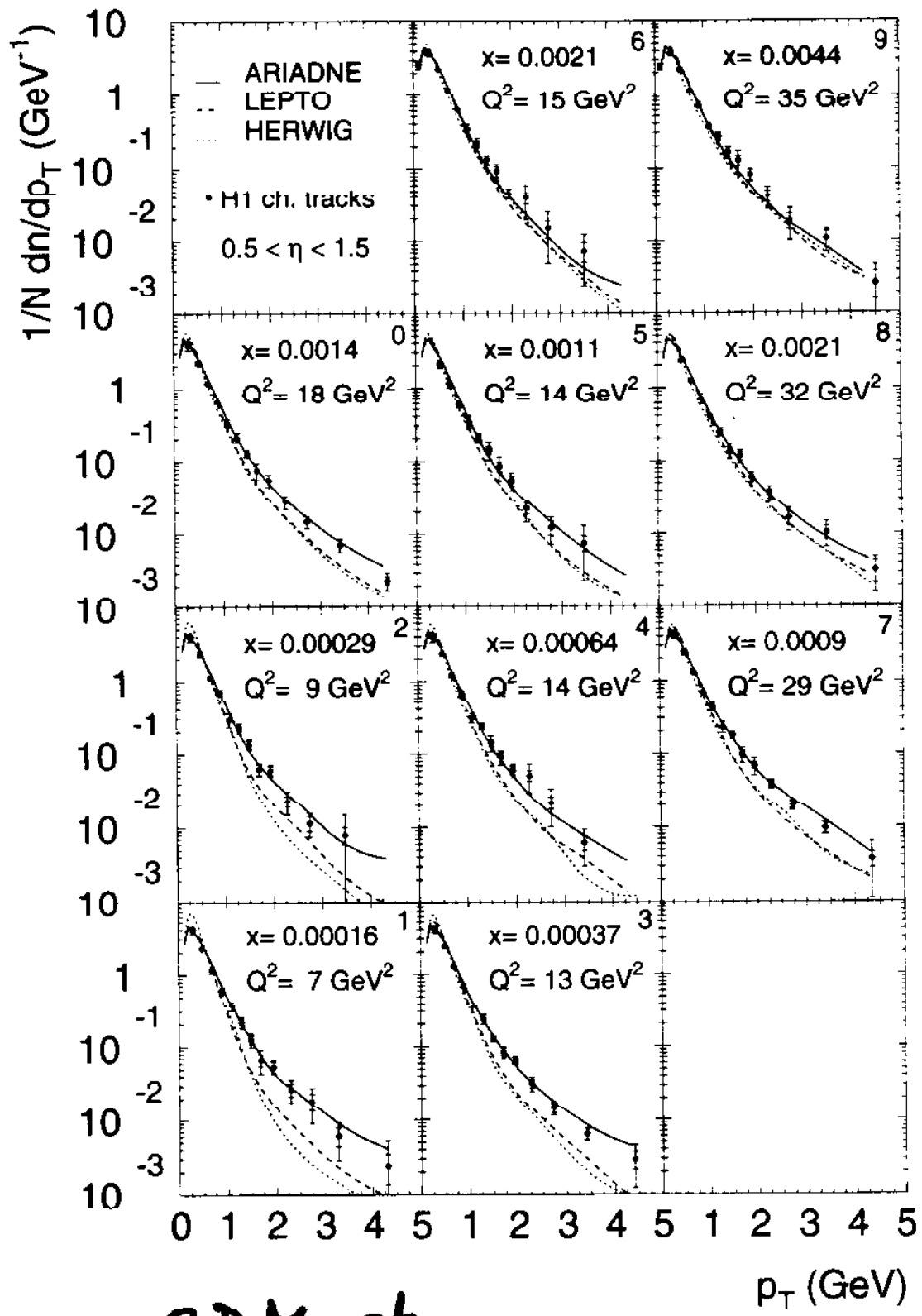
- First Analysis of DIS Event Shape Parameters
 $\langle 1 - T_c \rangle, \langle 1 - T_z \rangle, \langle B_c \rangle, \langle \rho_c \rangle$ in the Breit Current Hemisphere with the coverage of a large Range in $Q = 7 \div 100 \text{ GeV}$ in a Single Experiment
- The Event Shapes become more collimated with rising Q as expected. and give consistent results. They are compatible with a Universal Power Correction Parameter $\alpha_s \approx 0.5$ within $\pm 20\%$
- The Strong Coupling Constant $\alpha_s(M_Z)$ and $\bar{\alpha}_0$ are simultaneously determined independently of Fragmentation Models using C^2/α_s^2 . Calculations of DISENT and MEPJET
- The comparison with e^+e^- Experiments shows that the Q Dependence of Thrust and Jet Masses is in gross Agreement despite differences in the underlying Physics and the analysis methods. The same Power Correction Parameters α_s are found within $\pm 20\%$ of e^+p results.

BFKL effects in Hadronic Final State

- The Rise of F_2 at low x can be explained by DGLAP
- Can we observe BFKL behaviour with less inclusive observables?
 - E_T flow
 - Forward jet production
 - Charged particle p_T spectra
- At low x , the Next to Leading Order is not sufficient: triple gluon vertex dominates.
 - But do we need the BFKL resummation of $(\alpha_s \ln \frac{1}{x})^n$ terms?
 - Or is the DGLAP approach $((\alpha_s \ln \frac{Q^2}{Q_0^2})^n$ terms) precise enough?
- Problem: No complete simulation exists for BFKL. However the Colour Dipole Model (Ariadne) is expected to mimick the BFKL behaviour



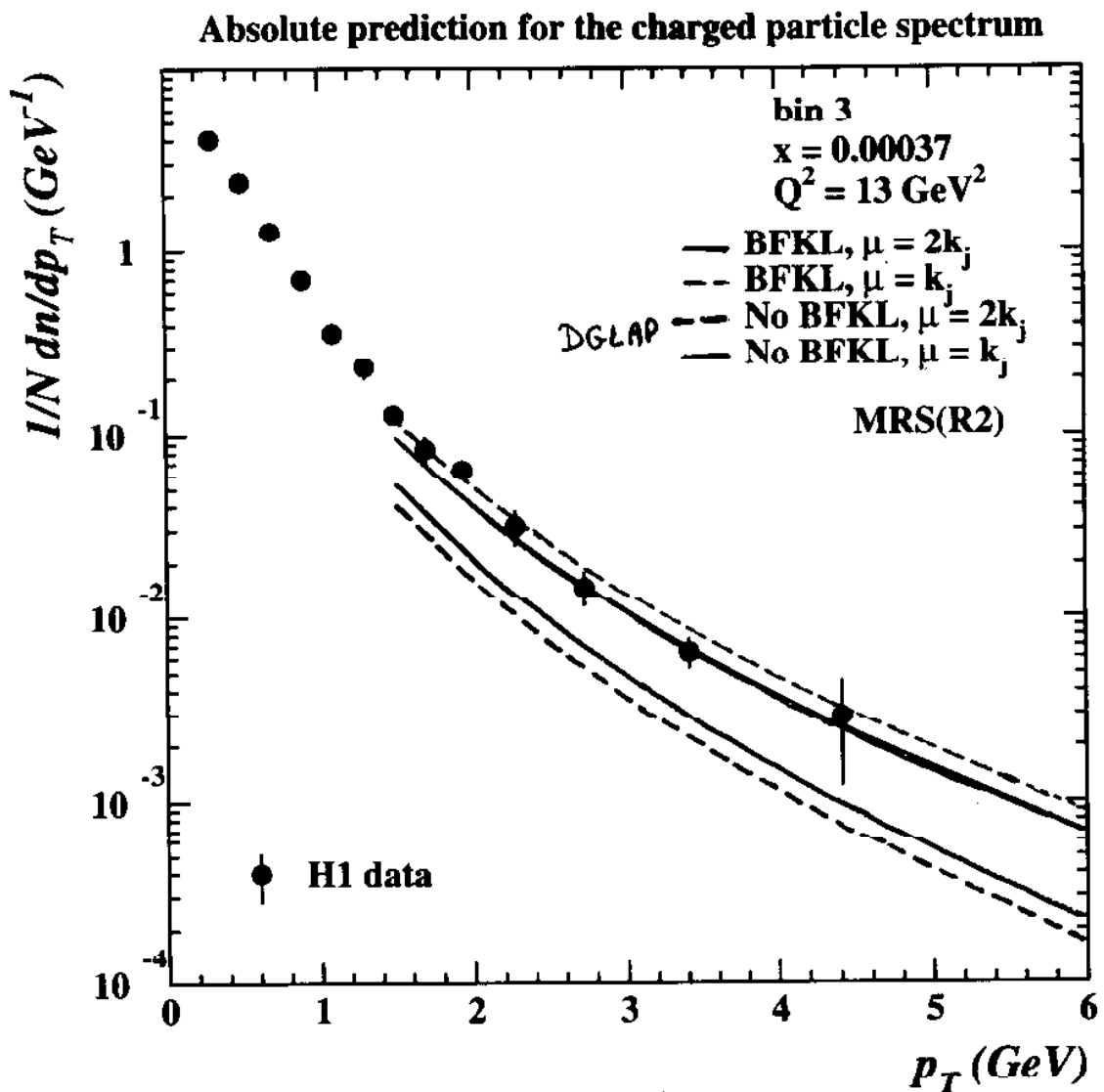
Transverse momentum spectra of Charged Particles



CDM ok

LEPTO/HERWIG undershoots at low x

BFKL: data vs theory

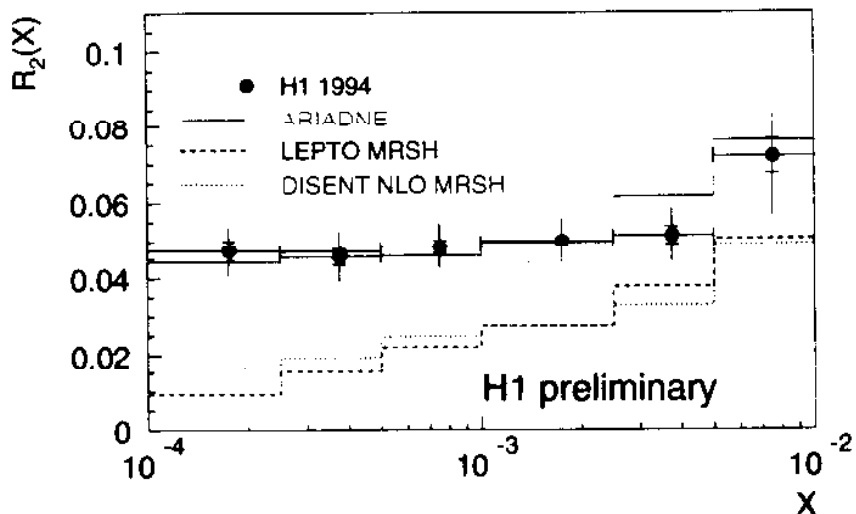
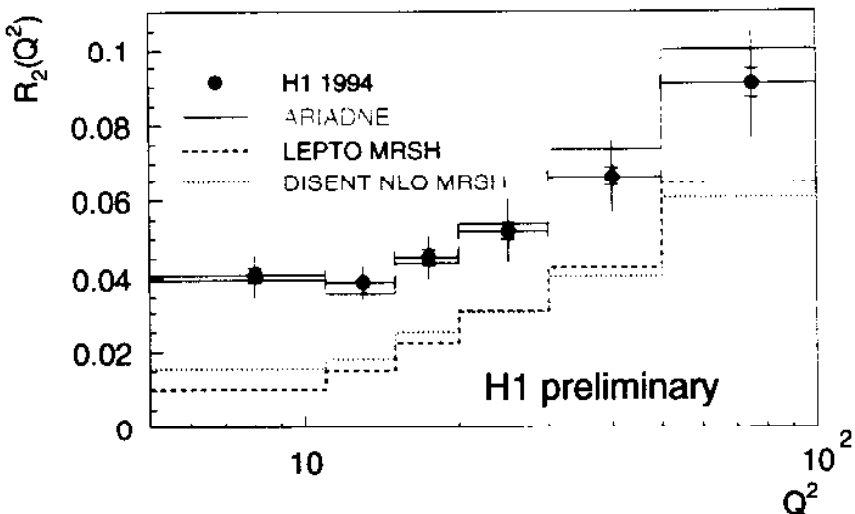


Kwiccinski, Lang, Martin

Dijet Rates

- DIS selection, cone algorithm in hadronic centre of mass
 $R_{\text{cone}} = 1.$ $p_t > 5 \text{ GeV}$
- Data corrected to the hadron level

$$R_{2\text{-jet}} = \frac{N_{2\text{-jet}}}{N_{\text{all}}}$$



- MEPS model and NLO calculation are not able to describe data

Structure Functions

In the single photon exchange approximation:

$$\frac{d^2\sigma}{dxdQ^2} = \frac{2\pi\alpha^2}{xQ^4} [(2(1-y) + y^2)F_2(x, Q^2) - y^2 F_L(x, Q^2)] \\ = \Gamma[\sigma_T(x, Q^2) + \epsilon(y)\sigma_L(x, Q^2)] \equiv \Gamma\sigma_{\gamma^* p}^{\text{eff}}(x, y, Q^2)$$

$$F_L = F_2 - 2xF_1, \quad R = \frac{\sigma_L}{\sigma_T} = \frac{F_L}{F_2 - F_L} \\ \Gamma = \frac{\alpha(2 - 2y + y^2)}{2\pi Q^2 x}, \quad \epsilon(y) = \frac{2(1 - y)}{2 - 2y + y^2}$$

- with 94 data: $\sim 2 - 3 \text{ pb}^{-1}$

$$\Rightarrow Q^2 = 1.5 - 5000 \text{ GeV}^2 \\ \Rightarrow y = 0.01 - 0.78$$

- with 95 data: $\sim 0.11 \text{ pb}^{-1}$ shifted vertex

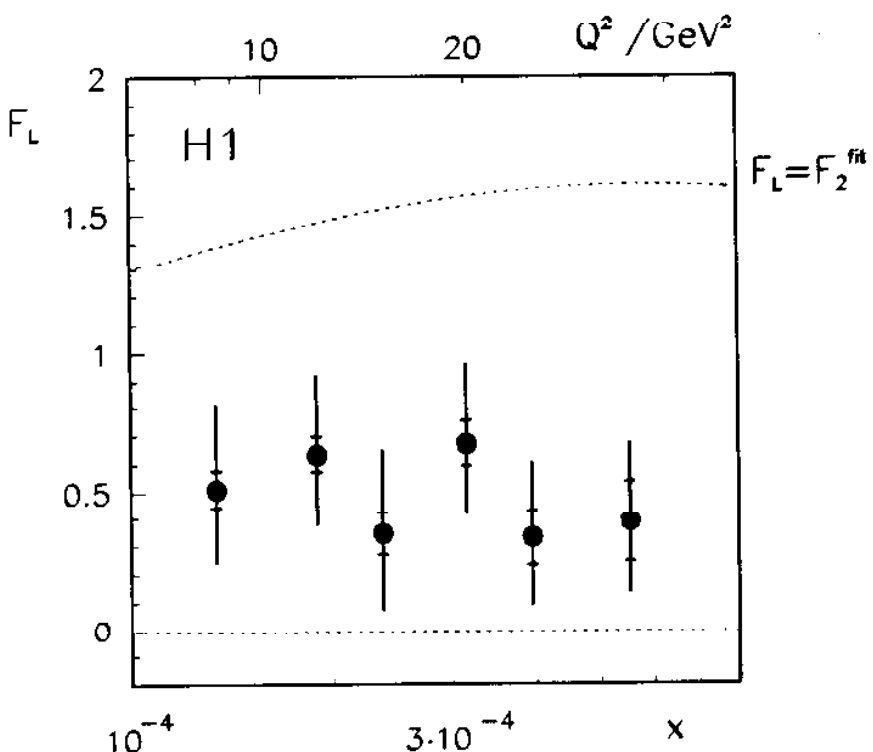
$$\Rightarrow Q^2 = 0.35 - 3.5 \text{ GeV}^2 \\ \Rightarrow y = 0.03 - 0.75$$

- F_L ?

The Longitudinal Structure Function

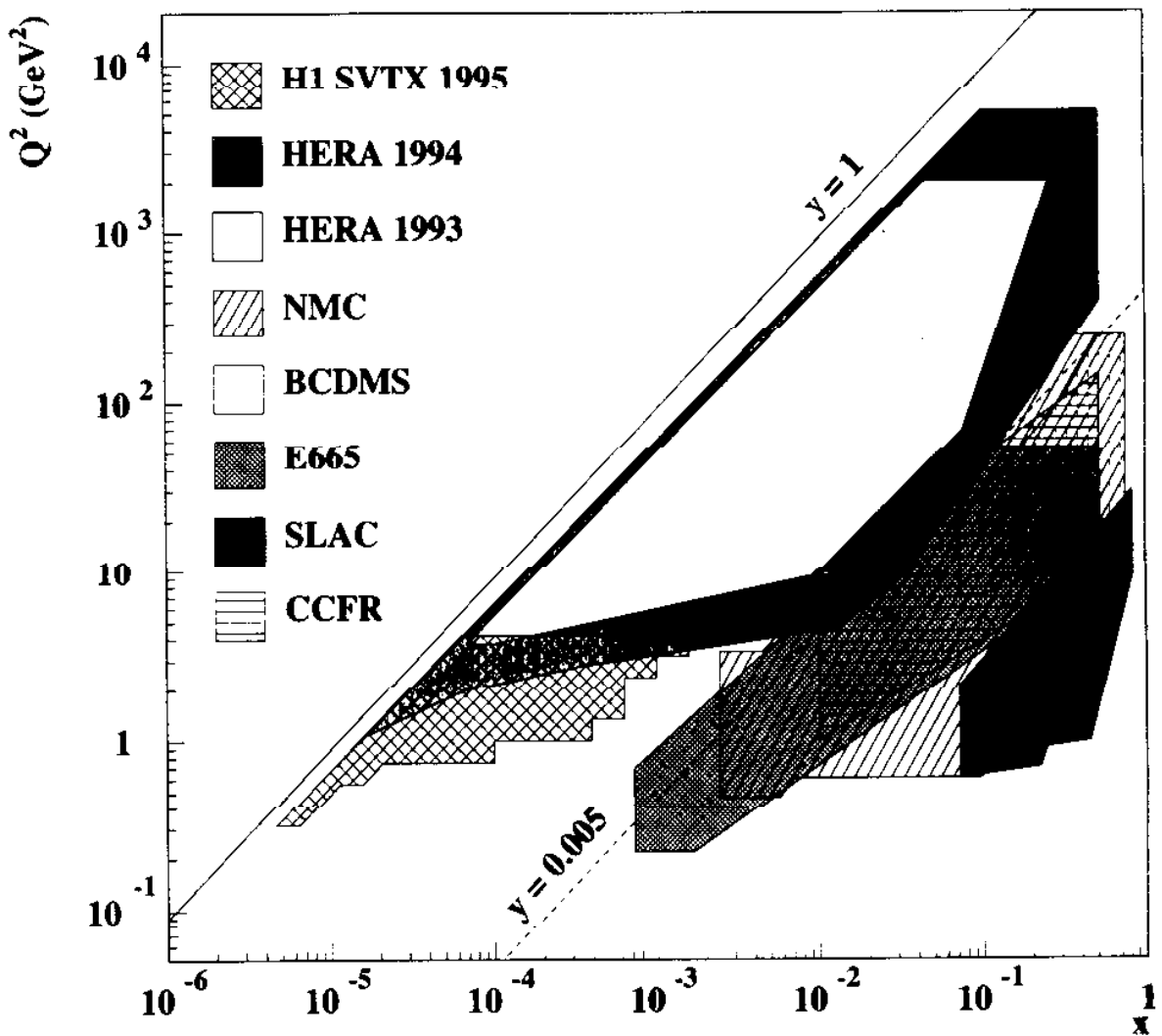
- Conventional Method:
 - measure $\sigma(x, Q^2)$ at different \sqrt{s}

- New Subtraction Method by H1:
 - measure $\sigma(x, Q^2)$ at high y
 - extrapolate F_2 with NLO DGLAP fit from the data at $y \leq 0.35$ up to $y = 0.7$
 - subtract F_2 part from $\sigma(x, Q^2) \Rightarrow F_L$

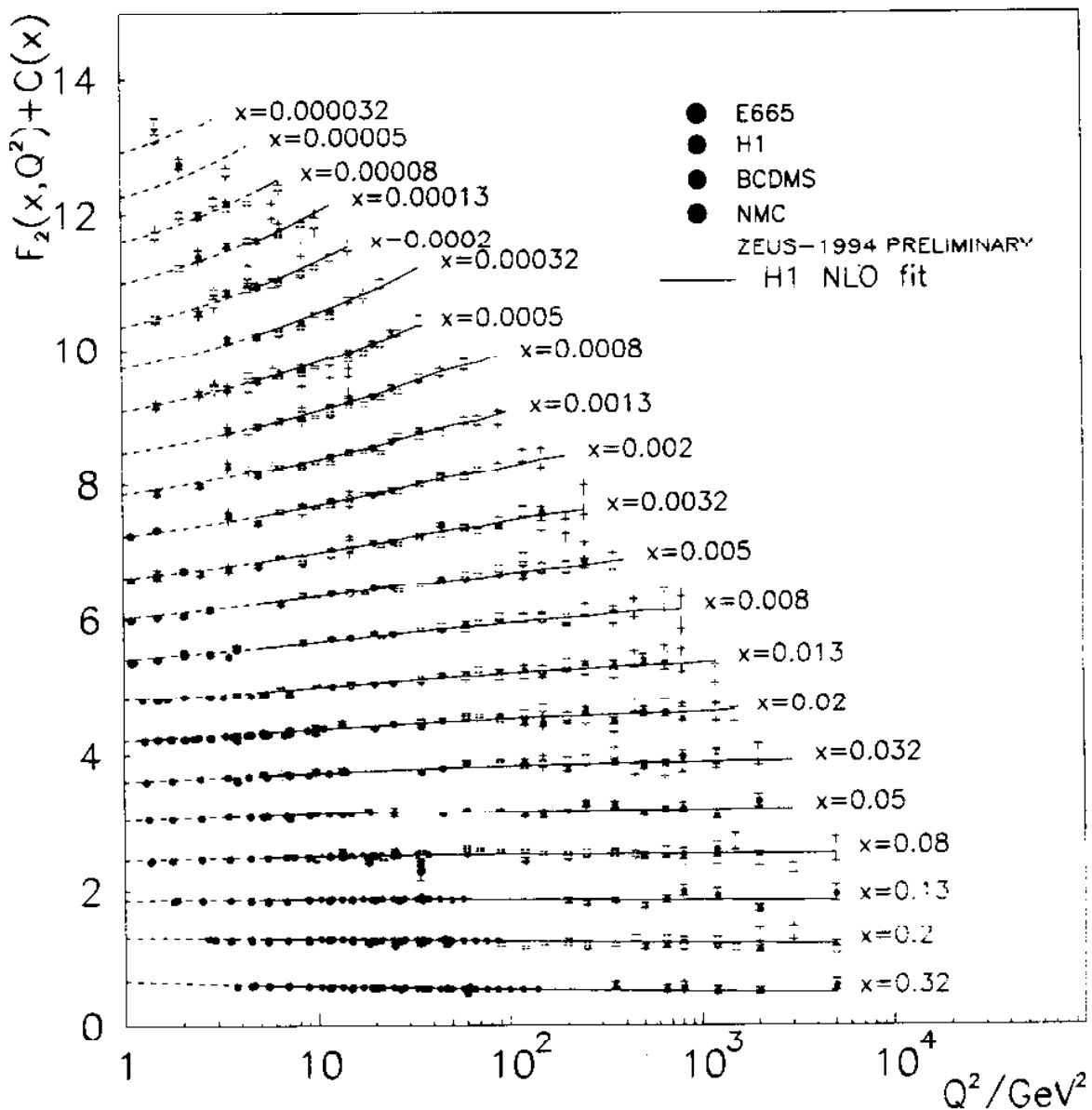


⇒ first determination of F_L at small x
 ⇒ F_L compatible with $F_2^{fit, fit}$ (Altarelli-Martinelli)

F_2^p in the (x, Q^2) Kinematic Plane



Scaling Violations

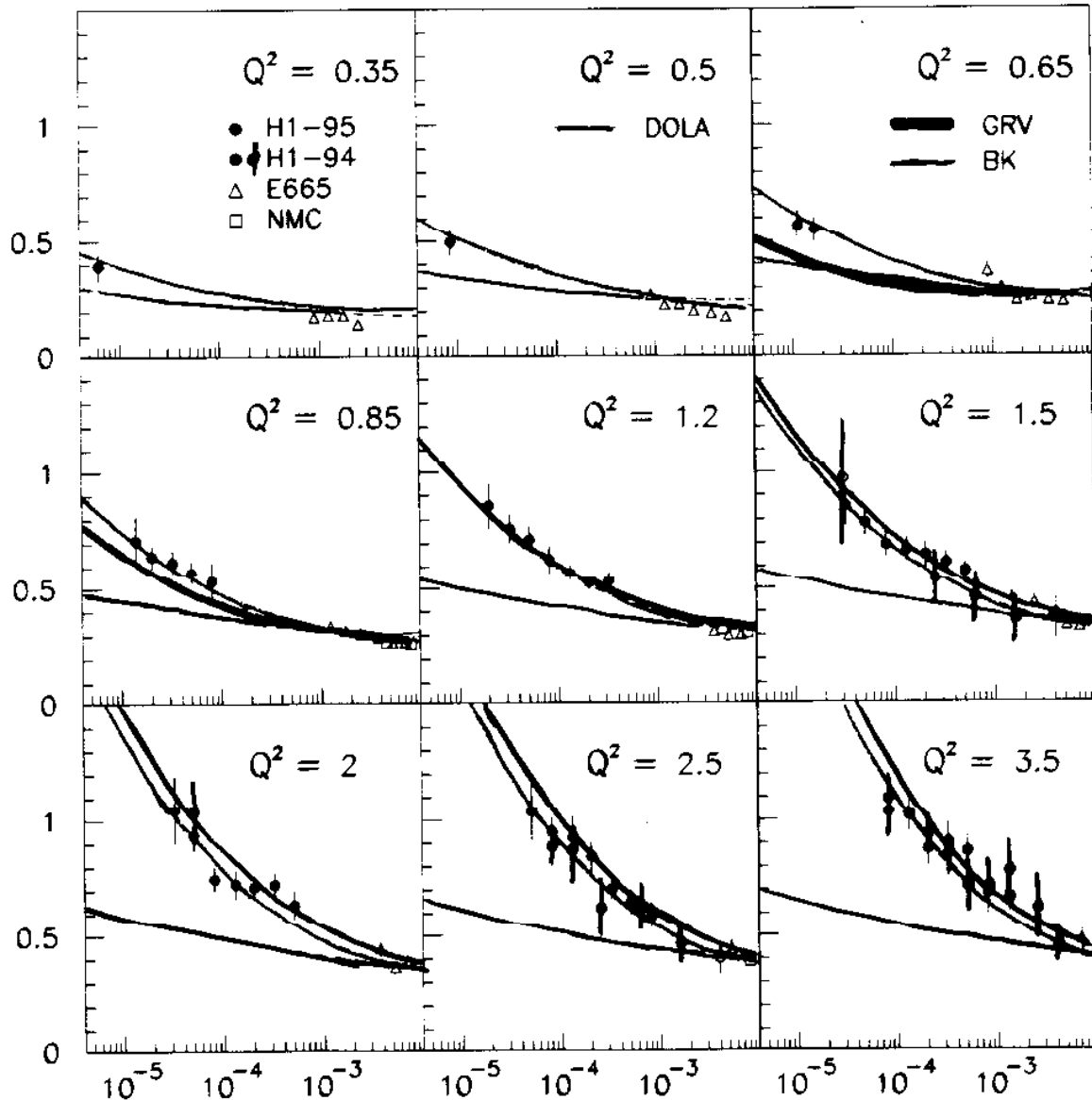


F_2 at low x and low Q^2

- DoLa: Assumption of Q^2 -independent Regge behaviour up to a few GeV^2 (Soft Pomeron)
- BK: Combination of GVMD Model with pQCD

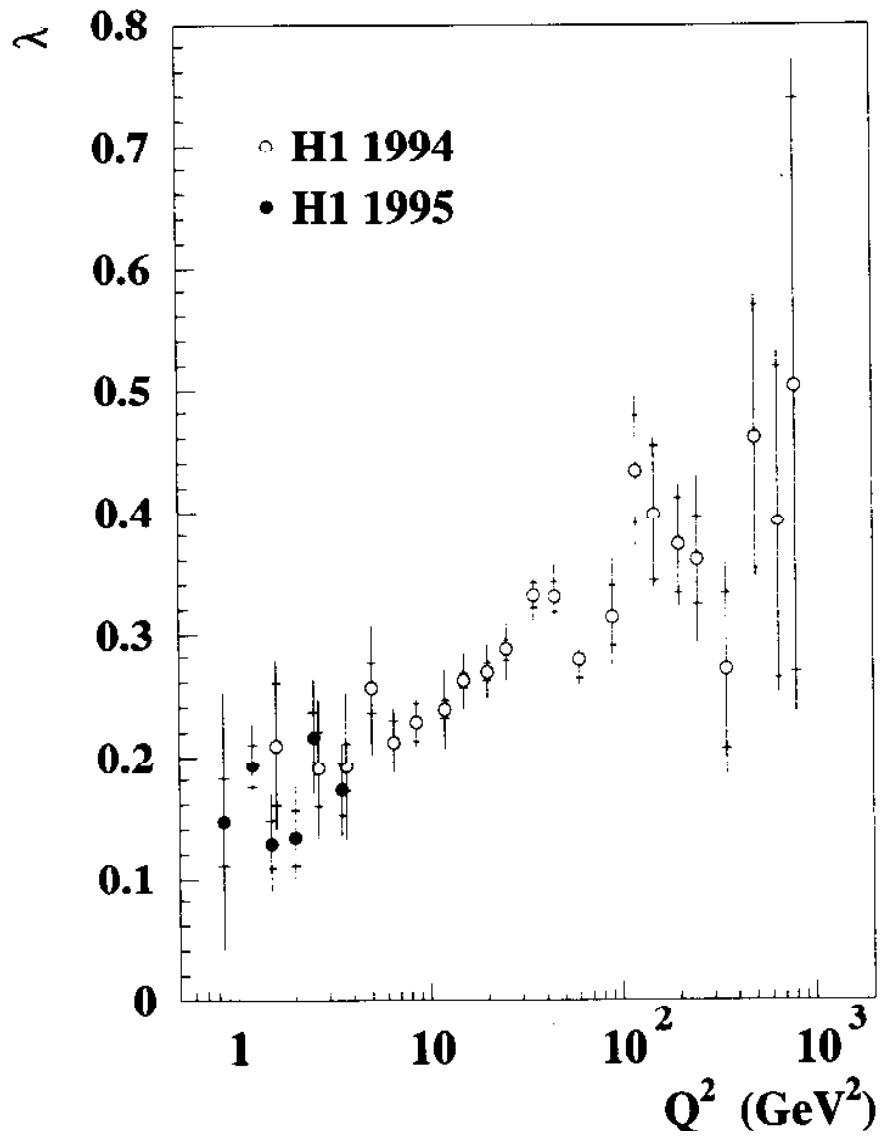
$$F_2(x, Q^2) = F_2^{\text{VMD}}(x, Q^2) + \frac{Q^2}{Q_0^2 + Q^2} F_2^{\text{QCD}}(\bar{x}, Q^2 + Q_0^2)$$

- GRV: pQCD evolution, NLO DGLAP. Valence like parton distribution at low starting scale 0.34 GeV^2 .

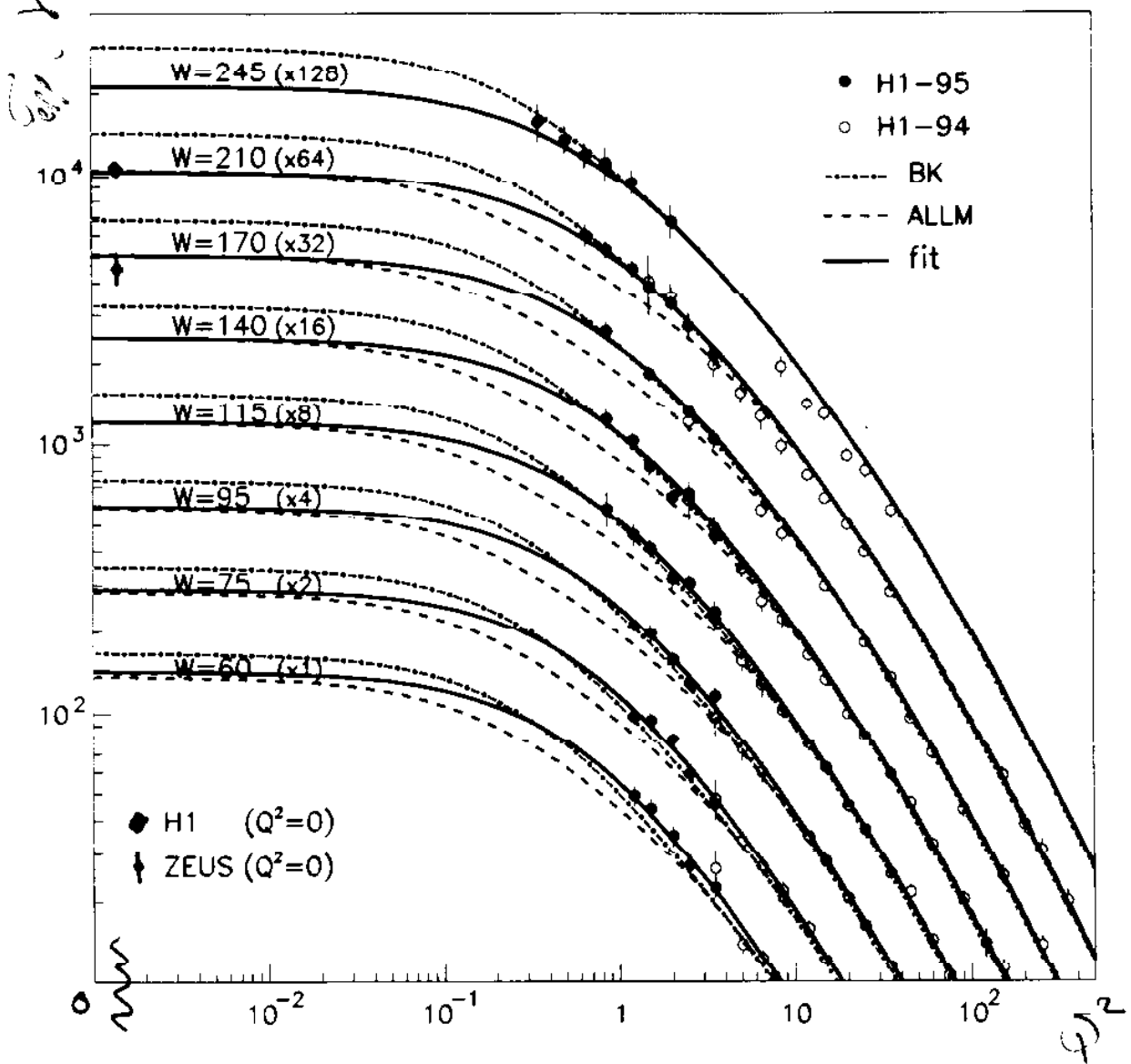


F_2 Rise at Low x

- fit $F_2(x, Q^2) \propto x^{-\lambda(Q^2)}$ in every Q^2 bin
⇒ tends towards $\lambda \simeq 0.08$ at $Q^2 \rightarrow 0$
- compatible with Double Asymptotic Scaling



$\gamma^* p$ – DIS Transition Region

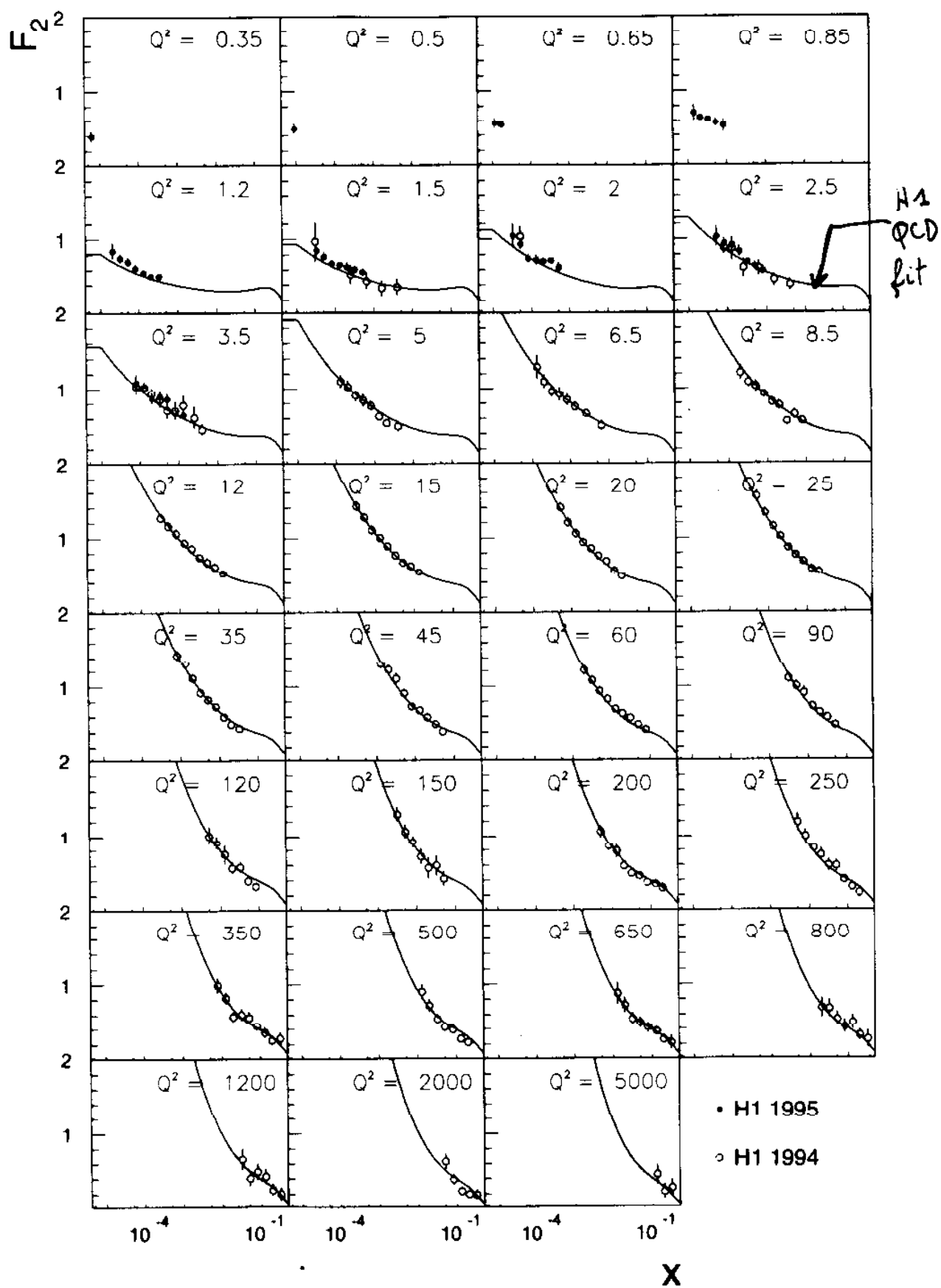


- Refit ‘BK’ to photoproduction points:

$$F_2(x, Q^2) = C_{VMD} \cdot F_2^{\text{VMD}}(x, Q^2) + \frac{Q^2}{Q_0^2 + Q^2} F_2^{\text{QCD}}(\bar{x}, Q^2 + Q_0^2)$$

$$C_{VMD} = 0.77, \quad Q_0^2 = 0.45 \text{ GeV}^2$$

H1 Results from 94 and 95 data



Summary on Structure Functions

- New measurement of $F_2(x, Q^2)$ with data recorded in 1995, using the new H1 Backward Detectors allows extension of the kinematic plane

$$Q^2 \geq 0.35 \text{ GeV}^2 \quad \text{and} \quad x \geq 6 \cdot 10^{-6}$$

- Transition from pQCD to non-perturbative region explored:
 - At $Q^2 \lesssim 1 \text{ GeV}^2$ pQCD fails to describe the data
 - At lowest Q^2 , F_2 approaches Regge expectation: dynamics in this region still to be understood
- The DGLAP equations allow an impressive description of the data in the full kinematic plane above $Q^2 \gtrsim 1 \text{ GeV}^2$
 - The gluon density has been shown to rise at low x
 - F_L has been determined at high y
- High precision F_2 measurement using 96 data in progress $\Rightarrow \alpha_s$

Cross Sections in DIS at High Q^2

NC: $e^\pm p \rightarrow e^\pm + X$

- $\mathcal{F}_1, \mathcal{F}_3$ Structure functions of the proton include Z^0 -propagators and ew-couplings
 \mathcal{F}_2 : contains the pure γ and Z' exchange.
 \mathcal{F}_3 : $\gamma - Z^0$ Interference term

$$\frac{d^2\sigma^{NC}(e^\pm p)}{dx dQ^2} = \frac{2\pi\alpha^2}{xQ^4} (Y_+ \mathcal{F}_2(x, Q^2) \mp Y_- x \mathcal{F}_3(x, Q^2))$$

$$Y_\pm = (1 \pm (1-y)^2)$$

CC: $e^+ p \rightarrow \bar{\nu} + X; e^- p \rightarrow \nu + X$

- e^+ and e^- allow to probe different valence quarks

$$\frac{d^2\sigma^{e^+ p}}{dx dQ^2} = \frac{G_\mu^2}{\pi} \frac{M_W^2}{(M_W^2 + Q^2)^2} ((\bar{u} + \bar{c}) + (1-y)^2(d+s))$$

$$\frac{d^2\sigma^{e^- p}}{dx dQ^2} = \frac{G_\mu^2}{\pi} \frac{M_W^2}{(M_W^2 + Q^2)^2} ((u + c) + (1-y)^2(d+\bar{s}))$$

$u = u(x, Q^2)$ momentum density of u quarks.

G_μ = Fermi-Coupling constant

Data Analysis:

- 94+95+96 data: $\simeq 14 \text{ pb}^{-1}$. Based on Positron and Hadrons; T. G. C. [Signature]
- 94+95 data: $\simeq 6 \text{ pb}^{-1}$. Based on Hadrons only.

C. S. Rie.
Rien WGI

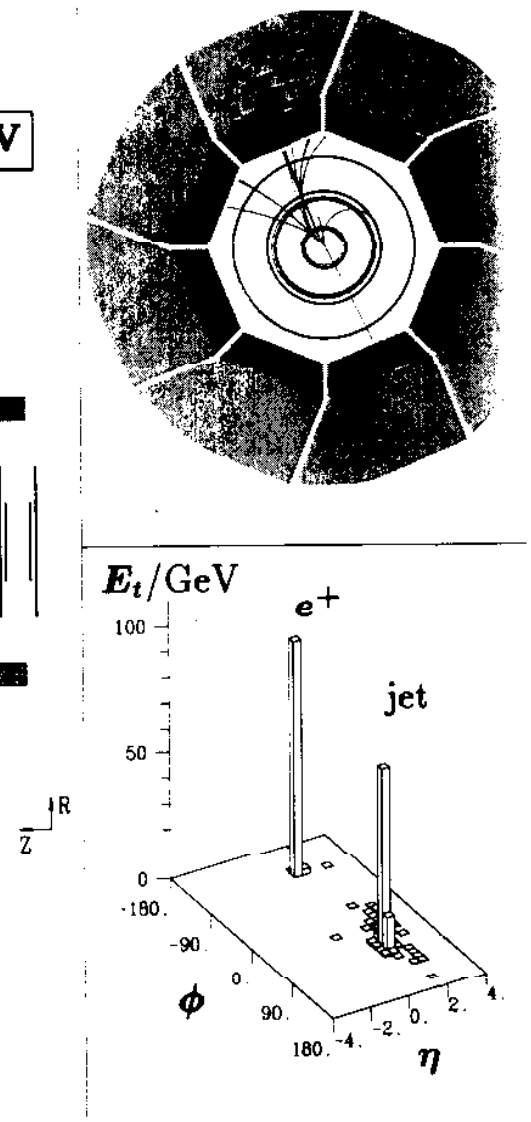
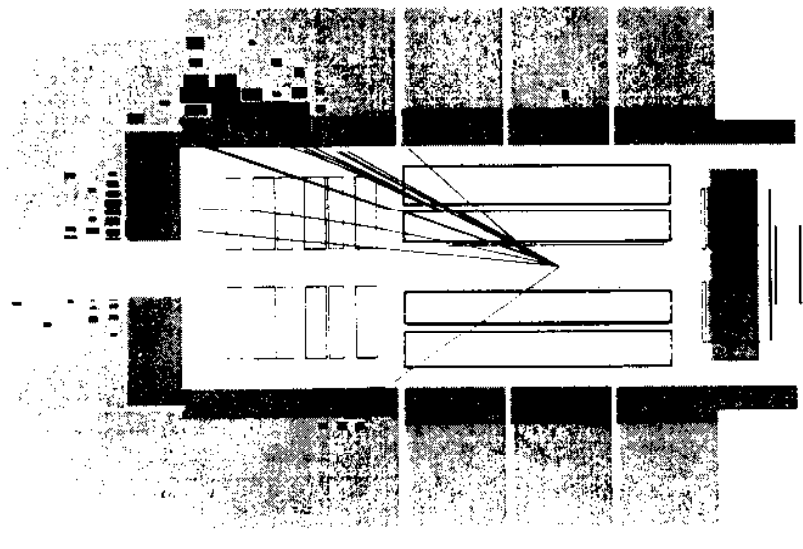
NC DIS Candidate

- 1

II Run 85528 Event 71329

Date 28/08/199

$$Q^2 = 16950 \text{ GeV}^2, \quad y = 0.44, \quad M = 196 \text{ GeV}$$



LAr Calorimetry

- Very fine granularity
(≈ 44000 cells)
 - Optimal for e -identification
 - Hadronic energy compensation
by offline weighting
- $\Delta\theta_e \sim 2\text{mrad}$ for $10^\circ < \theta_e < 30^\circ$
 $\Delta\theta_e \leq 5\text{mrad}$ for $30^\circ < \theta_e < 145^\circ$
 $\sigma(E)/E \simeq 12\%/\sqrt{E/\text{GeV}} \oplus 1\%$
 $\sigma(E)/E \simeq 50\%/\sqrt{E/\text{GeV}} \oplus 2\%$

Experimental errors :

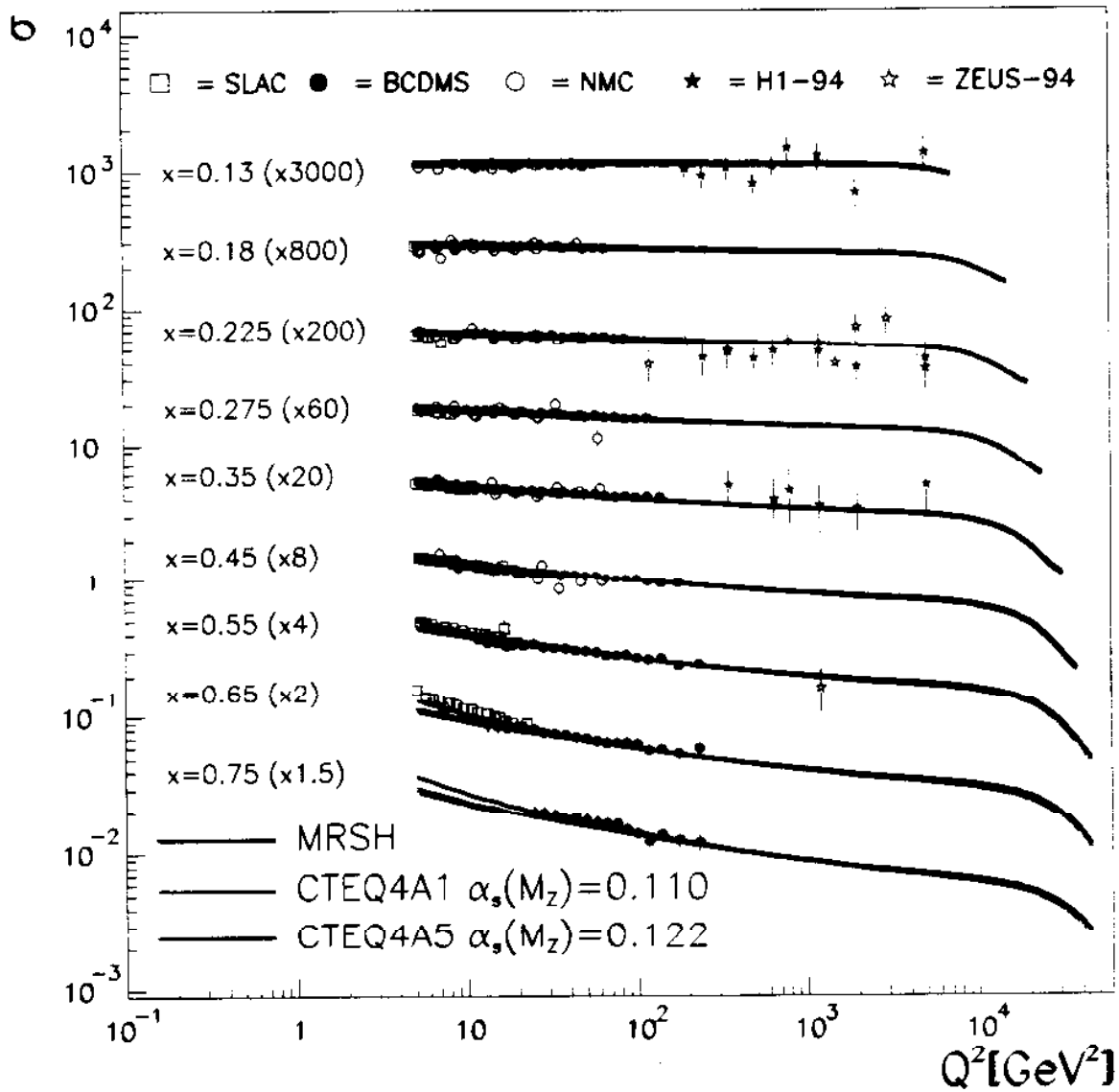
electromagnetic energy scale $\rightarrow \pm 3\%$ hadronic energy scale $\rightarrow \pm 1\%$

The Standard DIS Model

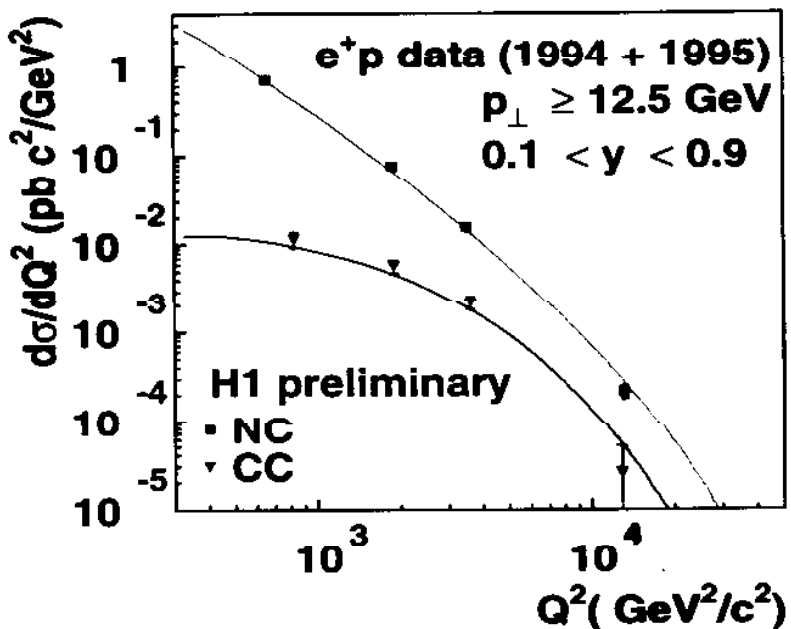
Expectation from NC and CC DIS →

- Parton Model (single γ , Z and W exchange)
 - Description of the proton in terms of scale dependent structure functions (SF) (F_L set to $\simeq 0$)
 - parton density parametrizations extracted from global fits of
 - Martin-Stirling-Roberts MRS (H)
 - SF Measurements at fixed target
BCDMS, NMC, CCFR, EMC, ...
 - + inclusive lepton + direct photon
WA70, E605, CDF, UA68, ...
 - + low Q^2 SF Measurements at HERA
H1, ZEUS
- Parton densities evolved to high Q^2 using next-to-leading order DGLAP equations
- “Theoretical” errors :
 - parton density distribution → $\pm 5\%$
 1. input data (e.g. BCDMS at high x and low Q^2)
 2. initial shapes of distributions
 - value of $\alpha_s \rightarrow \pm 4\%$
comparison CTEQ4 (A1) → (A5) and MRS (R1) → MRS (R2)
 - higher order QED corrections → $\pm 2\%$

Q^2 Evolution of the Neutral Current Cross-Section at High x



$d\sigma/dQ^2$ and $d\sigma/dy$ for NC and CC events



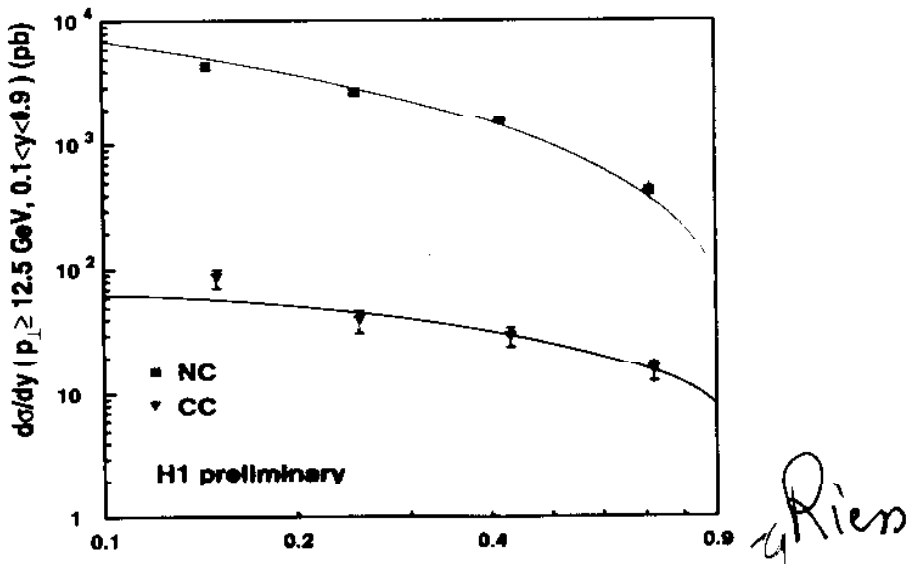
Total Cross Section for Charged Current e^+p :

Cuts: $p_t > 12.5 \text{ GeV}$ and $0.1 < y < 0.9$

$$\sigma_{\text{tot}}^{CC} = (25.2 \pm 2.5 \pm 0.8) \text{ pb} \quad (\text{H1 prelim.})$$

- Good agreement with the standard DIS model. NC and CC cross-sections have comparable size for $Q^2 \approx m_Z^2 \text{ GeV}^2$.
- CC cross section can disentangle valence from sea quarks

$$\frac{d^2\sigma^{CC}}{dx dQ^2} = \frac{G_F^2}{\pi} \frac{M_W^2}{(M_W^2 + Q^2)^2} (A(\bar{u} + \bar{c}) + B(1 - y)^2(d + s))$$



Event Selection

Neutral Current Selection

- electron identification:
 - shower shape test in calorimeter
 - isolation in $\eta - \phi$ cone ($R < 0.25$)
 - track matching the calorimeter cluster
- $E_{T,e} > 25\text{GeV}$ $\Theta_e > 10^\circ$
- $0.1 < y_e < 0.9$ $Q_e^2 > 2500\text{GeV}^2$
- momentum balance
 - transverse: $P_{T,\text{miss}}/\sqrt{E_T} < 3\sqrt{\text{GeV}}$
 - longitudinal: $43 < \sum E - P_z < 63\text{GeV}$
 $2E_e^\circ = 55\text{GeV}$ expected
cuts events with initial state radiation

Charged Current Selection

- $P_{T,\text{miss}} > 50\text{GeV}$
- $\frac{E_T - P_{T,h}}{E_T} < 0.5$

Remaining Background

- < 0.1% on full NC sample
- < 0.1 event at $Q^2 > 10000\text{ GeV}^2$
- dominating source: photoproduction of jet-jet events

Kinematic Reconstruction

- Electron Method:

$$y_e = 1 - \frac{E'_e}{E_e} \sin^2 \frac{\theta_e}{2} \quad Q_e^2 = 4 E'_e E_e \cos^2 \frac{\theta_e}{2}$$

- most precise at high y / low x
- degrades severely at low y

- Hadron Method:

$$y_h = \frac{\Sigma}{2E_e} \quad Q_h^2 = \frac{p_{t,h}^2}{1 - y_h}$$

- rather unprecise
- only method for charged current

- Σ Method:

$$y_\Sigma = \frac{\Sigma}{\underbrace{\Sigma + E'_e(1 - \cos\theta_e)}_{2 \cdot E_{\text{Initial State Radiation}}}} \quad Q_\Sigma^2 = \frac{E'^2_e \sin^2 \theta_e}{1 - y_\Sigma}$$

- precise over the whole kinematic range
- Independent of QED initial state radiation

- Double Angle Method:

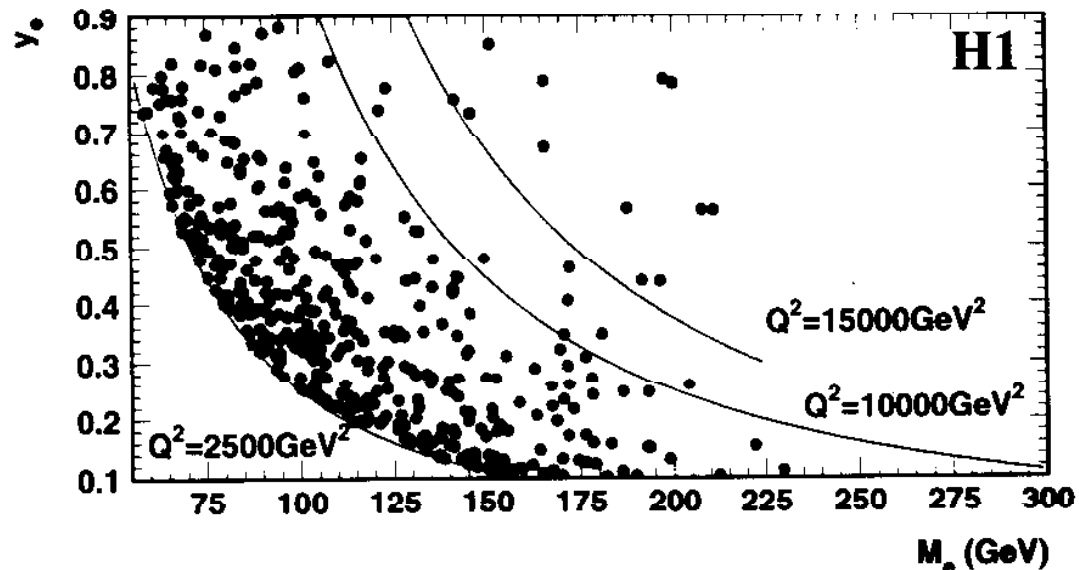
$$y_{DA} = \frac{\tan \gamma/2}{\tan \gamma/2 + \tan \theta/2} \quad Q_{DA}^2 = 4 E'^2_e \frac{\tan \theta}{2} \frac{\cot \theta/2}{\tan \gamma/2 + \tan \theta/2}$$

- high precision at high Q^2
- degrades at low Q^2 and sensitive to QED radiation

with

$$\Sigma = \sum_{\text{hadrons}} (E_h - p_{z,h}) \quad \tan \gamma/2 = \frac{\Sigma}{p_{t,h}}$$

NC Data Sample in the M - y Plane



NC DIS candidates e -method

$$0.1 < y_e < 0.9 \quad Q^2 > 2500 \text{ GeV}^2$$

Observed 443 events

Expected 427 ± 38 events

$$(N_{exp}/N_{gen} \sim 80\%)$$

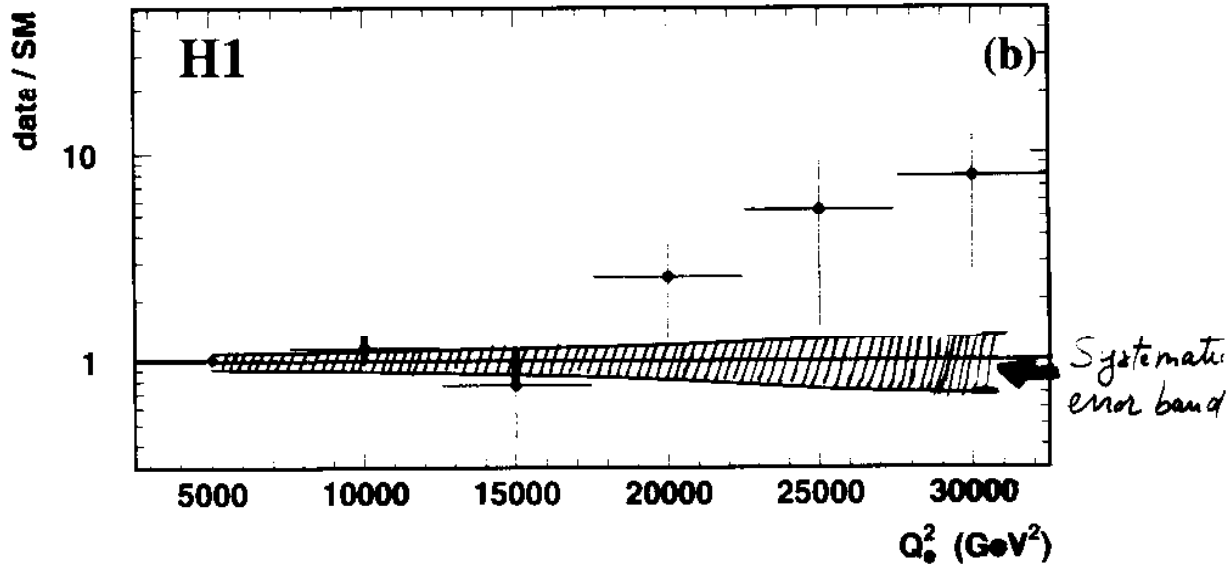
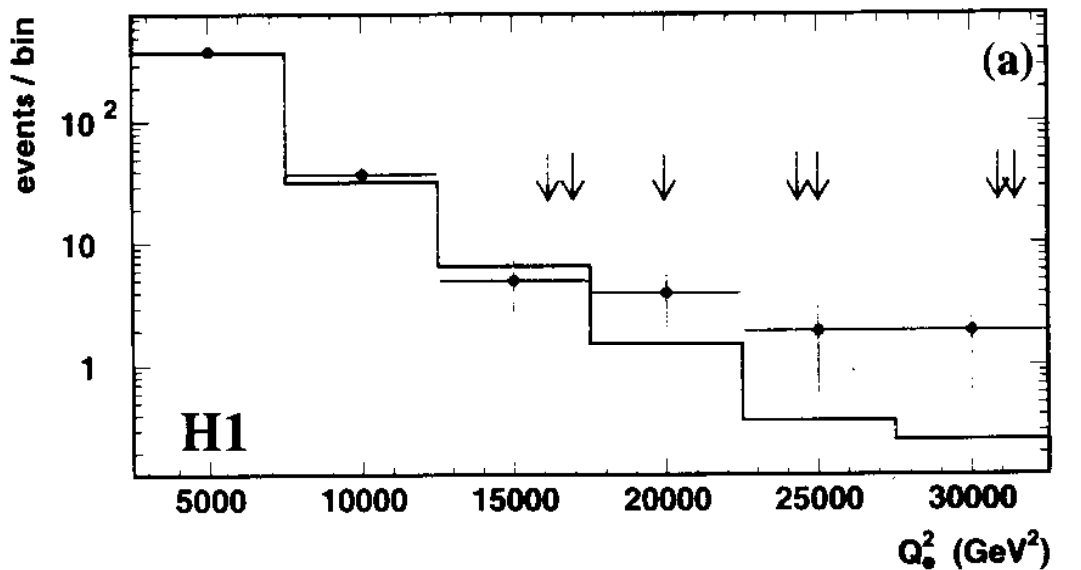
CC DIS candidates h -method

$$y_h < 0.9 \quad P_{T,h} > 50 \text{ GeV}$$

Observed 31 events

Expected 34.2 ± 5.8 events

Q^2 Dependence



Errors dominated by uncertainty on e.m. energy scale
~ 8.5% at low Q_e^2 ~ 30% at highest Q_e^2

High Q^2 Events with $Q^2 > Q_{min}^2$

Neutral Current

$Q_{min}^2(\text{GeV}^2)$	2500	10000	15000	20000	30000
N_{obs}	443	20	12	5	2
N_{DIS}	426.7 ± 38.4	18.3 ± 2.4	4.71 ± 0.76	1.32 ± 0.27	0.23 ± 0.05
$\mathcal{P}(N \geq N_{obs})$	0.35	0.39	6×10^{-3}	1.4×10^{-2}	2.3×10^{-2}

Poisson probability that
number of expected events \geq number of observed events:

$$\mathcal{P}(N \geq N_{obs}) = \int_0^{+\infty} dx G(x; b, \delta b) \sum_{k=N_{obs}}^{\infty} p(k; x)$$

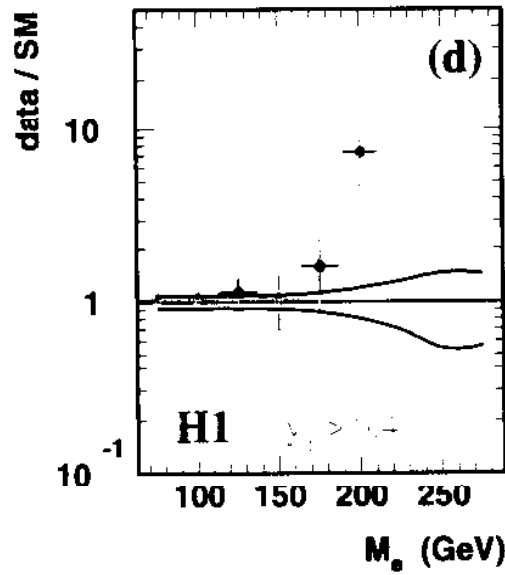
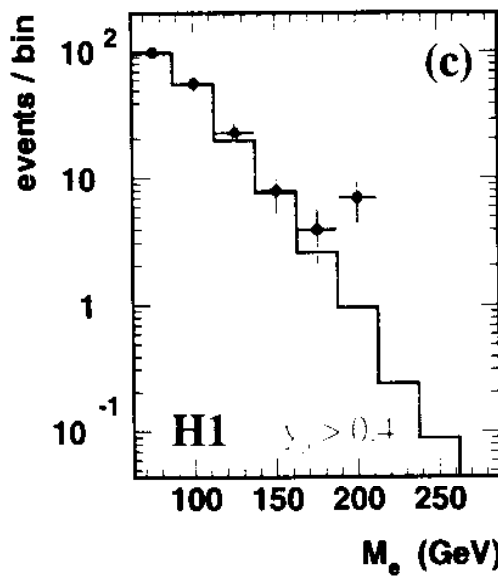
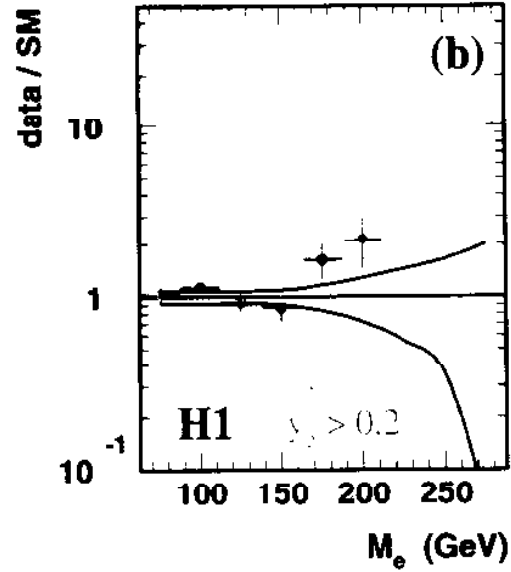
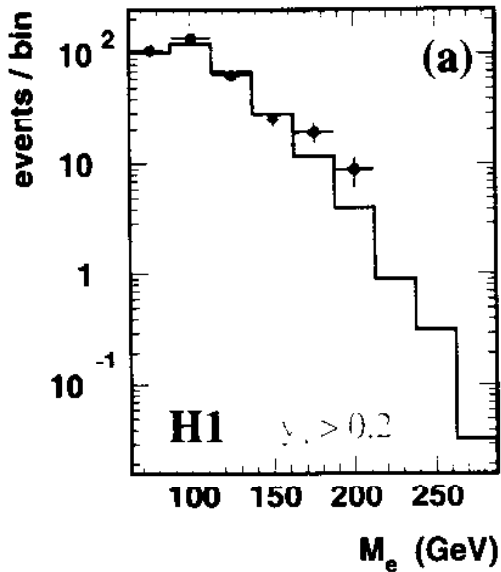
where:

- $p(k; x)$ = Poisson probability to observe k events for x expected events.
- $G(x; b, \delta b)$: Gaussian smearing of mean expected number of events with systematic error on expectation.

Charged Current

$Q_{min}^2(\text{GeV}^2)$	2500	5000	10000	15000	20000
N_{obs}	31	24	10	4	3
N_{DIS}	34.2 ± 5.8	21.1 ± 4.2	5.07 ± 1.88	1.77 ± 0.87	0.74 ± 0.39
$\mathcal{P}(N \geq N_{obs})$	0.64	0.31	7×10^{-2}	0.14	5.4×10^{-2}

Mass Dependence



- Excess seen at highest mass

- More visible at large y_e

High Mass, High y events

- The 7 Neutral Current events with $M > 180$ GeV mass and $y > 0.4$ are kinematically consistent between Electron, Double-Angle and Electron+Jet methods:
Electromagnetic/Hadronic calibration is OK from the data
- Further Check is provided with comparison to the Sigma method, which is independent of QED radiation. The mass average of the 7 events is stable within 1% between these 2 methods.

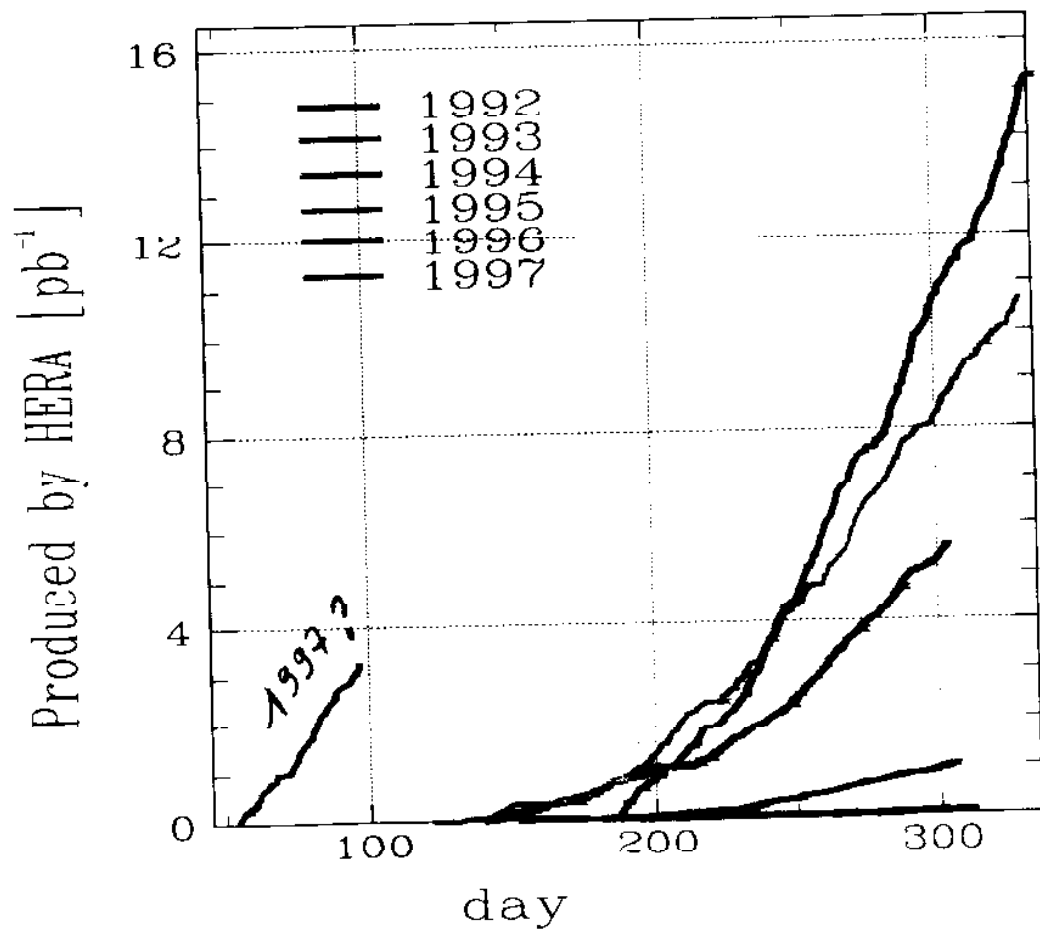
event	M (GeV)	M_Σ (GeV)	y_e	y_Σ	Q_e^2 (GeV 2)	Q_Σ^2 (GeV 2)
1	196	196	0.439	0.443	16950	17100
	± 5		$\pm .014$		± 360	
2	208	209	0.563	0.592	24350	25930
	± 4		$\pm .012$		± 430	
3	188	188	0.566	0.561	19950	19760
	± 12		$\pm .032$		± 1400	
4	198	196	0.790	0.786	30870	30230
	± 2		$\pm .008$		± 530	
5	211	210	0.562	0.525	25030	23120
	± 4		$\pm .012$		± 440	
6	192	190	0.440	0.501	16130	18140
	± 6		$\pm .016$		± 400	
7	204	202	0.783	0.786	31420	31940
	± 7		$\pm .008$		± 540	

High Q^2 Summary

- For $Q^2 < 15000\text{GeV}^2$, the Q^2 , M and y distributions are well reproduced by the expectations from standard Neutral Current and Charged Current processes
 - For $Q^2 > 15000\text{GeV}^2$:
12 Neutral Current observed, 4.71 ± 0.76 are expected, i.e.
 $\mathcal{P}(N \geq N_{obs}) = 6 \times 10^{-3}$;
 - The excess of observed events in the M and y plane is most prominent at $M = 200\text{GeV} \pm 12.5\text{GeV}$ and $y > 0.4$:
7 NC events observed, 0.95 ± 0.18 are expected
Probability for comparable or larger excess anywhere in the M and y region considered = $\mathcal{O}(1\%)$
 - The excess cannot be accounted for by:
 - detector effects
 - parton densities compatible with existing data
 - α_s variations, higher order corrections
 - Only explanation found:
statistical fluctuation or new physics
- need more data

Prospects

A bright future!



Integrated Luminosity

Prospects

